Molecular Phylogenetics and Evolution 102 (2016) 20–29

Contents lists available at ScienceDirect

Molecular Phylogenetics and Evolution

journal homepage: www.elsevier.com/locate/ympev

Phylogenomics, biogeography and diversification of obligate mealybug-tending ants in the genus *Acropyga*

Bonnie B. Blaimer [a,*], John S. LaPolla [b], Michael G. Branstetter [a,c], Michael W. Lloyd [a], Seán G. Brady [a]

[a] Department of Entomology, National Museum of Natural History, Smithsonian Institution, Washington, DC 20560, USA
[b] Department of Biological Sciences, Towson University, Towson, MD 21252, USA
[c] Department of Biology, University of Utah, Salt Lake City, UT 84112, USA

ARTICLE INFO

Article history:
Received 10 February 2016
Revised 19 May 2016
Accepted 23 May 2016
Available online 24 May 2016

Keywords:
Ultraconserved elements
UCEs
Insect systematics
Mutualism
Herding

ABSTRACT

Acropyga ants are a widespread clade of small subterranean formicines that live in obligate symbiotic associations with root mealybugs. We generated a data set of 944 loci of ultraconserved elements (UCEs) to reconstruct the phylogeny of 41 representatives of 23 *Acropyga* species using both concatenation and species-tree approaches. We investigated the biogeographic history of the genus through divergence dating analyses and ancestral range reconstructions. We also explored the evolution of the *Acropyga*-mealybug mutualism using ancestral state reconstruction methods. We recovered a highly supported species phylogeny for *Acropyga* with both concatenation and species-tree analyses. The age for crown-group *Acropyga* is estimated to be around 30 Ma. The geographic origin of the genus remains uncertain, although phylogenetic affinities within the subfamily Formicinae point to a Paleotropical ancestor. Two main *Acropyga* lineages are recovered with mutually exclusive distributions in the Old World and New World. Within the Old World clade, a Palearctic and African lineage is suggested as sister to the remaining species. Ancestral state reconstructions indicate that Old World species have diversified mainly in close association with xenococcines from the genus *Eumyrmococcus*, although present-day associations also involve other mealybug genera. In contrast, New World *Acropyga* predominantly evolved with *Neochavesia* until a recent (10–15 Ma) switch to rhizoecid mealybug partners (genus *Rhizoecus*). The striking mandibular variation in *Acropyga* evolved most likely from a 5-toothed ancestor. Our results provide an initial evolutionary framework for extended investigations of potential co-evolutionary interactions between these ants and their mealybug partners.

1. Introduction

Acropyga ants are best known for their obligate relationship with root mealybugs (Rhizoecidae, following Hodgson, 2012), on which they evidently depend on completely for food through the production of honeydew by the mealybugs (Schneider and LaPolla, 2011; Williams, 1998). These small subterranean formicine ants occupy leaf litter, soil and rotten wood throughout most of the world's tropics. Worker ants display a range of morphological adaptations probably associated with their subterranean lifestyle, such as a yellow, thin cuticle covered by a thick layer of pubescence, short scapes with reduced antennal segmentation, and very small eyes (Bünzli, 1935; LaPolla, 2004; Weber, 1944). The relationship of *Acropyga* with their symbionts is maintained by alate queens vertically transmitting mealybugs among nests during their mating flights, a unique behavior among herding ants that LaPolla et al. (2002) termed trophophoresy. An alate ant queen will select a mealybug, grasping it between her mandibles while she flies and mates. The individual mealybug carried by the queen serves as a seed individual for the new colony of mealybugs that will be tended by the offspring of the queen (LaPolla, 2004; Williams, 1998). Not surprisingly, trophophoresy is rarely observed, with only a handful of anecdotal observations of mating swarms (Brown, 1945; Bünzli, 1935; Buschinger et al., 1987; Eberhard, 1978; Prins, 1982). In the few cases that mealybugs carried by the queens have been examined, these were always adult gravid females (LaPolla and Spearman, 2007; Smith et al., 2007; Taylor, 1992; Terayama, 1988; Williams and LaPolla, 2004).

The mealybug family Rhizoecidae associated with *Acropyga* consists of two subfamilies: the Xenococcinae, all of which are obligately associated with *Acropyga*, and the Rhizoecinae, of which only a few are obligately associated with *Acropyga*. This trophobi-

* Corresponding author.
E-mail addresses: bonnieblaimer@gmail.com (B.B. Blaimer), jlapolla@towson.edu (J.S. LaPolla), mgbranstetter@gmail.com (M.G. Branstetter), lloydm@si.edu (M.W. Lloyd), bradys@si.edu (S.G. Brady).

http://dx.doi.org/10.1016/j.ympev.2016.05.030
1055-7903/

otic association has great potential in becoming a model system for the study of symbiosis in general and specifically in the evolution of ant agriculture. Ant agriculture can be broken into two broad categories: fungus-growers and herders (Ivens, 2015). While there have been many studies on the fungus-growing ants (e.g. Hölldobler and Wilson, 2011; Mehdiabadi and Schultz, 2010), remarkably few have addressed ants that herd scale insects (Coccoidea) and aphids (Aphidoidea). The study of herder ants offers the opportunity to investigate the evolution and maintenance of an animal-to-animal mutualistic symbiosis. Trophophoresy in this system results in vertical transmission of mealybugs across ant generations, providing the possibility that at least some degree of cospeciation has occurred between the two participants, as found in other insect-symbiont systems (e.g. Degnan et al., 2004; Kikuchi et al., 2009).

Such tight mutualistic associations over evolutionary time could also lead to morphological adaptation in one or both partners (Shingleton et al., 2005). In *Acropyga*, one of the most intriguing morphological characteristics is the extraordinary variability observed in the mandibles. Fig. 1A–F depicts a range of *Acropyga* mandible forms, demonstrating the variation seen in mandibular teeth count (from 3 to 9 teeth) and the overall shape of the mandible (from triangular to more elongate and curved). Few ant genera display such a range in mandibular form. In the predatory dacetine ants, for example, a similarly large range of mandible variation has been linked to specialization to the type of prey these ants capture (Bolton, 2000). Given that both *Acropyga* workers and queens extensively manipulate the mealybugs with their mandibles, it seems likely that this mandibular variation plays an important role in this symbiotic relationship.

Previous phylogenetic studies on *Acropyga* ants were either based on morphological data alone (LaPolla, 2004), or on very few molecular markers (LaPolla et al., 2006). The latter study also suffered from limited taxon sampling, as its main objective was to confirm the monophyly and position of *Acropyga* within formicines. A recently published study, focused on Papua New Guinean *Acropyga* species and a population genetic analysis of *A. acutiventris* (Janda et al., 2016), was also based on few genetic markers. To improve our understanding of *Acropyga* evolutionary relationships world-wide, we used phylogenomic methods based on ultraconserved elements (UCEs) to reconstruct a robust species-level phylogeny of the genus. UCEs are a group of molecular markers increasingly used in phylogenomic studies (Crawford et al., 2015; Faircloth et al., 2012; Smith et al., 2014), and have been successfully employed for higher-level systematics of ants and other Hymenoptera (Blaimer et al., 2015; Faircloth et al., 2015). The UCE method represents a targeted enrichment phylogenomic approach in which highly conserved orthologous fragments can be captured and sequenced from the genomes of distantly related taxa. While ultraconserved core regions of UCEs remain preserved across broad evolutionary distances, these are flanked by more variable regions, thereby rendering these markers also useful for species-level studies (Smith et al., 2013).

We use this target-capture and multiplexed sequencing approach to obtain 944 UCE loci for 23 species of *Acropyga* ants. We analyze these data using a traditional concatenation approach, as well as recently developed statistical binning and species tree methods. We also estimate a time-calibrated phylogeny using a subset of 100 UCE loci and use these results to investigate the biogeographic history of *Acropyga* by reconstructing ancestral biogeographic ranges. To explore hypotheses about the evolution of the mutualism of *Acropyga* ants with rhizoecid mealybugs, we correlate mealybug associations with our phylogeny and investigate mandibular tooth count as a trait potentially under selection in this partnership.

2. Materials and methods

2.1. Taxon sampling

Our data set comprised 41 *Acropyga* specimens representing 23 of 40 currently valid species. We further included nine closely related Formicinae outgroup taxa from a recent UCE phylogeny for that subfamily (Blaimer et al., 2015). One *Acropyga* specimen could not be confidently identified to species level, representing either one of the very closely related species *A. decedens* or *A. goeldii*. We treat this species with uncertain identity as a combination

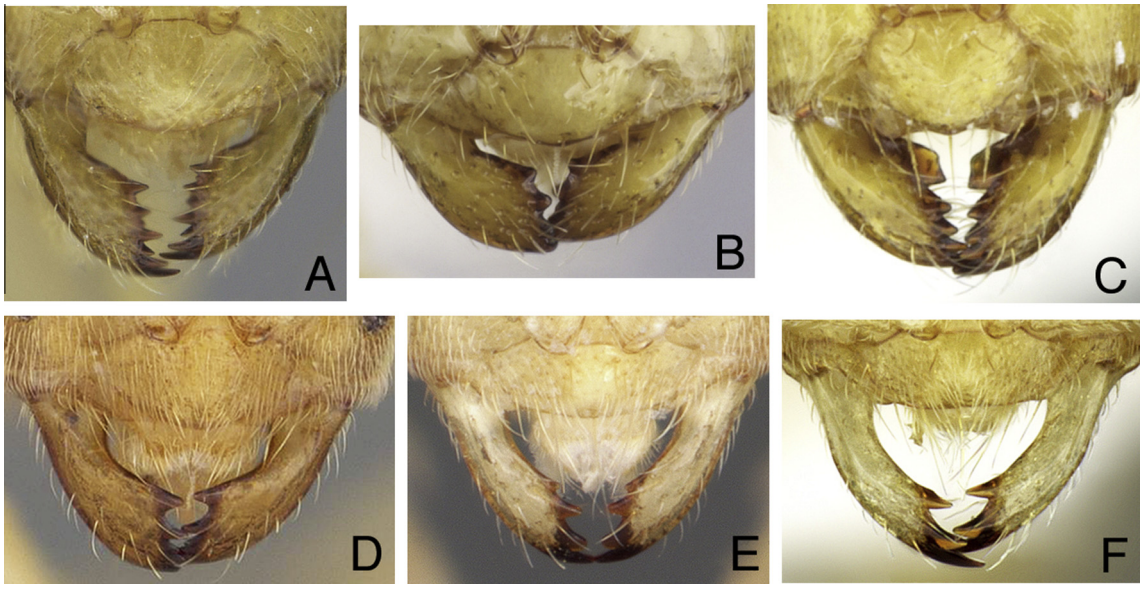

Fig. 1. Diversity of *Acropyga* mandibles. All images are from www.antweb.org; specific photographers are noted after each species. (A) *A. arnoldi* (CASENT0235249) (photo: Shannon Hartman); (B) *A. donisthorpei* (CASENT0249916) (photo: Will Ericson); (C) *A. butteli* (CASENT0906270) (photo: Estella Ortega); (D) *A. ayanganna* (USNMENT00413391) (photo: Jeffrey Sosa-Calvo); (E) *A. epedana* (CASENT0006064) (photo: April Nobile); (F) *A. exsanguis* (INBIOCRI001253903) (photo: Estella Ortega). All species except for *A. exsanguis* are included in the present study.

from the two species under consideration (*A. decedens*/*goeldii*). All specimens included in this study were collected in accordance with local regulations and all necessary permits were obtained. Voucher specimens have been deposited at the National Museum of Natural History (USNM collection; see Table S1 for specimen identifiers and collection data).

2.2. Molecular data collection

DNA was extracted destructively or non-destructively (specimen retained after extraction) from worker ants or pupae using a DNeasy Blood and TissueKit (Qiagen, Valencia, CA, USA). We quantified DNA for each sample using a Qubit fluorometer (High sensitivity kit, Life Technologies, Inc.) and sheared 1.8–245 ng (91 ng mean) DNA to a target size of approximately 500–600 bp by sonication (Q800, Qsonica LLC.), and used this sheared DNA as input for a modified genomic DNA library preparation protocol following Faircloth et al. (2015; but see supplementary methods). We enriched each pool using a set of 2749 custom-designed probes (MYcroarray, Inc.) targeting 1510 UCE loci in Hymenoptera (see Faircloth et al., 2015). We followed library enrichment procedures for the MYcroarray MYBaits kit (Blumenstiel et al., 2010), except we used a 0.1× concentration of the standard MYBaits concentration, and added 0.7 μL of 500 μM custom blocking oligos designed against our custom sequence tags. We used the with-bead approach for PCR recovery of enriched libraries as described in Faircloth et al. (2015). Following post-enrichment PCR, we purified resulting reactions using 1.0× speedbeads and rehydrated the enriched pools in 22 μL Elution Buffer.

We quantified post-enrichment library concentration with qPCR using a SYBR® FAST qPCR kit (Kapa Biosystems) on a ViiA™ 7 (Life Technologies), and based on the size-adjusted concentrations estimated by qPCR, we pooled libraries at equimolar concentrations and size-selected for 250–800 with a BluePippin (SageScience). The pooled libraries were sequenced using two partial lanes of a 150-bp paired-end Illumina HiSeq 2500 run (U Cornell Genomics Facility). Quality-trimmed sequence reads generated as part of this study are available under submission SRP069792 from the NCBI Sequence Read Archive (www.ncbi.nlm.nih.gov/sra/SRP069792). A detailed description of molecular methods can be found in the supplementary methods.

2.3. Processing and alignment of UCE data

We trimmed the demultiplexed FASTQ data output for adapter contamination and low-quality bases using Illumiprocessor, (Faircloth, 2013: http://dx.doi.org/10.6079/J9ILL), based on the package Trimmomatic (Bolger et al., 2014). All further data processing relied on the PHYLUCE package (Faircloth, 2016; but see also Faircloth et al., 2012); a detailed description of this pipeline and its scripts can be found in the supplementary methods.

We computed summary statistics on the data and assembled the cleaned reads using Trinity (version trinityrnaseq_r20140717) (Grabherr et al., 2011). To identify contigs representing enriched UCE loci from each species, species-specific contig assemblies were aligned to a FASTA file of all enrichment baits (min_coverage = 50, min_identity = 80), and sequence coverage statistics (avg, min, max) for contigs containing UCE loci were calculated. We created FASTA files for each UCE locus containing sequence data for taxa present at that particular locus and aligned these using MAFFT (Katoh et al., 2009) (min-length = 20, no-trim). We trimmed our alignments using Gblocks (Castresana, 2000) with relaxed settings. We selected a subset of UCE alignments for further analyses that had 70% taxon completeness for each locus ($\geqslant$35 of 50 taxa), thus retaining 944 UCE loci.

2.4. Phylogenetic inference

We selected data partitions using a development version of PartitionFinder (Frandsen et al., 2015) that depends on the software fast_TIGER (http://dx.doi.org/10.5281/zenodo.12914) and is designed to handle large genome-scale data sets. The UCE data set was analyzed with Maximum Likelihood (ML) best tree and bootstrap searches (N = 100) in RAxML v8.0.3 (Stamatakis, 2006). We also reconstructed gene trees for the 944 UCE loci by performing RAxML analyses (best tree and 200 bootstraps) on individual loci. Based on calculations of average bootstrap support for each gene tree in R (scripts by M. Borowiec available at https://github.com/marekborowiec/metazoan_phylogenomics/blob/master/gene_stats.R) we filtered these data to a subset of 100 loci with the highest average bootstrap score across all nodes in the gene tree ("UCE-100-best"), to use in dating analyses. We also selected two sets of 100 loci randomly to test against potential bias in the UCE-100-best data set. We further performed weighted statistical binning following Bayzid et al. (2015) on the full data of 944 UCE loci. This approach uses bootstrap-supported gene trees estimated from every locus in a data set to assign these loci into bins by assessing whether gene trees have conflicting or compatible branches (Bayzid et al., 2015). We used a support threshold of 50, above which branches of a tree are considered reliable (versus being present due to estimation error). After bin assignment, we concatenated all loci assigned to one bin into 'supergene alignments' (N = 209) and estimated bootstrap trees from these supergenes using RAxML. For bins with only one assigned locus (N = 525), we retained previously estimated gene trees. Species tree analyses with multilocus bootstrapping (Seo, 2008) (N = 200) were then performed in ASTRAL-II (Mirarab and Warnow, 2015) using 525 gene and 209 supergene trees. We performed this analysis both with and without the "species map" option, which is used to assign multiple individuals of the same species to one taxon. All of the above phylogenetic analyses were performed on the Smithsonian Institution high performance cluster (SI/HPC), or on an iMac desktop computer. Data matrices as well as tree files are deposited in the Dryad data repository (http://www.datadryad.org) with the http://dx.doi.org/10.5061/dryad.f4857.

2.5. Dating analyses and ancestral range reconstructions

We inferred divergence dates within *Acropyga* from a reduced 25-taxa set (one representative of each 23 species and the two most closely related outgroups) and a subset of "100-best" UCE loci (as described above), with the program BEAST v1.8 (Drummond et al., 2012), run via the SI/HPC. Analyses incorporated data partitioning (using models of sequence evolution GTR+I+G and GTR+I for nine subsets as estimated by PartitionFinder) and consisted of four runs each, with a chain length of 162–182 million generations. We employed a Yule tree prior and defined calibration priors on three nodes in the phylogeny (see Table 1). We tested whether these priors actually resulted in the desired posterior distributions on the respective nodes, by also performing the analysis without data, sampling

Table 1
Calibration points used for dating analyses in BEAST. Calibration priors were defined by using results (median height and 95% HPD intervals) estimated in a comprehensive analysis of the subfamily Formicinae (Blaimer et al., 2015), and by incorporating fossil information (LaPolla, 2005).

Calibration	Prior distribution	5%	Offset	Median	95%
Stem *Acropyga*	Lognormal	39.85	15	50	63.77
Agraulomyrmex-Formicinae genus01	Normal	12.44			38.76
Old World *Acropyga* clade	Normal	10			38

only from the prior ("empty"). We employed a diffuse gamma distribution on the mean branch lengths (ucld.mean; alpha = 0.001, beta = 1000), but otherwise left all remaining priors at their default values. Trace files were analyzed in Tracer v1.6 to determine chain convergence and burnin. After discarding a burnin of 25–30%, 55,793 tree files were then summarized with LogCombiner v1.8.2 and TreeAnnotator v1.8.2. Lineage-through-time plots were estimated in Tracer v1.6 from these post-burnin trees. We also performed BEAST analyses (with the same settings as above) on the two randomly selected sets of 100 UCE loci; here, we ran chains for 100–200 million generations and summarized 25,000–40,000 trees.

To evaluate the biogeographic history of the genus, we constructed a species distribution matrix for *Acropyga* (see Table S2). We used the resulting set of trees and the respective MCC tree from our BEAST analysis on the UCE-100-best data set to estimate ancestral ranges with the statistical dispersal-extinction-cladogenesis model (S-DEC, "Bayes-Lagrange", (Beaulieu et al., 2013)) implemented in the program RASP (Yu et al., 2015). We optimized estimations over a set of 1000 trees, randomly chosen from the set of 55,793 trees. As recommended by the authors of RASP (Yu et al., 2015) and practiced in other studies (e.g. Federman et al., 2015; Economo et al., 2015), outgroups were removed from the sample of MCC input trees before the analyses. We designated seven biogeographic areas (Neotropical, Nearctic, Palearctic, Afrotropical, Oriental, Indo-Australian and Australasian, sensu Bolton (1995)) and defined dispersal constraints based on the level of connectivity between these landmasses (see Table S3). The maximum number of possible areas for each state was set = 3 and we included all possible range combinations in the analysis. We incorporated missing biogeographic range information from one species absent from our phylogeny, *A. palearctica*, which is distributed in southern Europe. Based on the morphology of male genitalia, this species is sister to *A. arnoldi* (LaPolla, 2006), and we therefore coded the African *A. arnoldi* as Afrotropical + Palearctic (see Table S2). We did not include range information from any other species absent from our phylogeny because these were consistent with the ranges and relationships of the represented taxa.

2.6. Trait analyses

We investigated mandible evolution and associations of *Acropyga* species with mealybugs by inferring ancestral state reconstructions. We created a trait matrix (Table S2), scoring all 23 *Acropyga* species for (1) mandibular tooth count and (2) generic associations with mealybugs (following Schneider and LaPolla, 2011). Character data for the individual with uncertain identity represented a combination from the two species under consideration (*A. decedens* and *A. goeldii*), as we strongly assume these to be sister taxa. We used the *rayDISC* function in the R package *corHMM* (https://www.R-project.org/) which can analyze multivariate, polymorphic traits. Ancestral state reconstructions were hereby performed under the equal rates model (*ER*, one transition rate), the symmetric model (*SYM*, forward and reverse transition have the same rate) and the 'all rates different' model (*ARD*) on the time-calibrated tree by BEAST (100-best tree). We compared the fit of these models to the evolution of each of the three characters by performing a likelihood ratio test on the resulting –ln L scores (1-*pchisq*($\Delta - \ln L, df$)). We also performed these analyses while excluding data from the species with uncertain identity (*A. decedens/goeldii*).

3. Results

3.1. UCE capture results

Multiplexed sequencing of UCEs resulted in an average of 1.4 million reads per sample (see Table S4) with an average length of 315 base pairs (bp). An average of 18,226 contigs with a mean length of 375.7 bp were assembled by Trinity after adapter- and quality-trimming, with an average coverage of 19.7×. From all of the assembled contigs, we recovered an average of 945 UCE loci per sample with a mean length of 884 bp. The average coverage per captured UCE locus was 88.5×. Concatenation of the 944 loci (UCE-944) and the UCE-100-best subset generated matrices with a length of 733,400 bp and 91,396 bp respectively, whereas the two randomly chosen subsets had a length of 72,091 bp (random-1) and 80,443 bp (random-2).

3.2. Phylogeny

PartitionFinder divided our complete UCE-944 data set into 21 data subsets, and our UCE-100-best data set into nine data subsets; the random-1 and random-2 subsets were divided into 13 and 17 partitions, respectively. Phylogenetic results from partitioned ML bootstrap and best tree searches on the concatenated UCE-944 data set are depicted in Fig. 2. We recovered a highly resolved phylogeny for the genus *Acropyga* with most nodes displaying 100% bootstrap support. Only five nodes were recovered with a bootstrap score (BS) lower than BS = 96, mainly involving intraspecific relationships within *A. acutiventris*. The base of *Acropyga* consists of two well-supported clades. One of these clades comprises species only occurring in the New World (e.g., *A. epedana*, *A. donisthorpei*), whereas the other one includes exclusively species from the Old World (e.g., *A. acutiventris*, *A. arnoldi*) (Fig. 2). Our analyses further indicate a distinct Palearctic/African lineage within the Old World *Acropyga* (including *A. silvestrii*, *A. arnoldi*, and an undescribed species) as sister to the remainder of the Old World species from the Oriental, Indo-Australian and Australian regions.

Statistical weighted binning partitioned our 944 UCE gene trees into 733 bins: 525 bins of one locus, 208 bins of two loci, and one bin of three loci. The species tree estimated by ASTRAL-II from these 733 gene and supergene trees is very similar to the tree estimated in the concatenated analysis, with most nodes showing 100% bootstrap support (Fig. 3). This analysis maps individuals to their respective species and thus depicts only interspecific relationships. The two interspecific nodes with low support in the concatenated analysis also receive lowered support in the species tree analysis, although BS values are slightly improved (concatenated: BS = 59 and BS = 53, species tree: BS = 68 and BS = 77; see Fig. 3).

3.3. Biogeographic history

We performed Bayesian inference on our UCE-100-best data set using BEAST. The resulting phylogenetic tree is highly supported and similar to the one estimated from the concatenated and species tree approaches analyzing the full UCE-944 data set, with two exceptions (Fig. 4 and Table 2). First, BEAST recovered *A. silvestrii* as sister to the undescribed *Acropyga* species (posterior probability [PP] = 0.97), and second, the position of *A. myops* differs between these analyses, although with poor support in each.

Our dating analyses estimate a median age for the genus *Acropyga* of ca. 30 Ma (node 45, Table 2 and Fig. 4). The biogeographic origin of the genus remains uncertain, with a fairly widespread ancestor inhabiting the Neotropical, Palearctic and Indo-Australian regions receiving highest probability (Table 2, see also Table S5). Estimated crown-group ages for the Old World and New World clades are very similar, with 28.4 Ma and 27.8 Ma, respectively (node 33 and 44, Table 2 and Fig. 4). Ancestral distribution for the New World clade is unambiguously reconstructed as Neotropical, whereas the most recent common ancestor (MRCA) of the Old World clade is estimated to have had a distribution throughout the Palearctic and Indo-Australian region (but with only 57.5% PP, node 33, see Table 2). Most of the species

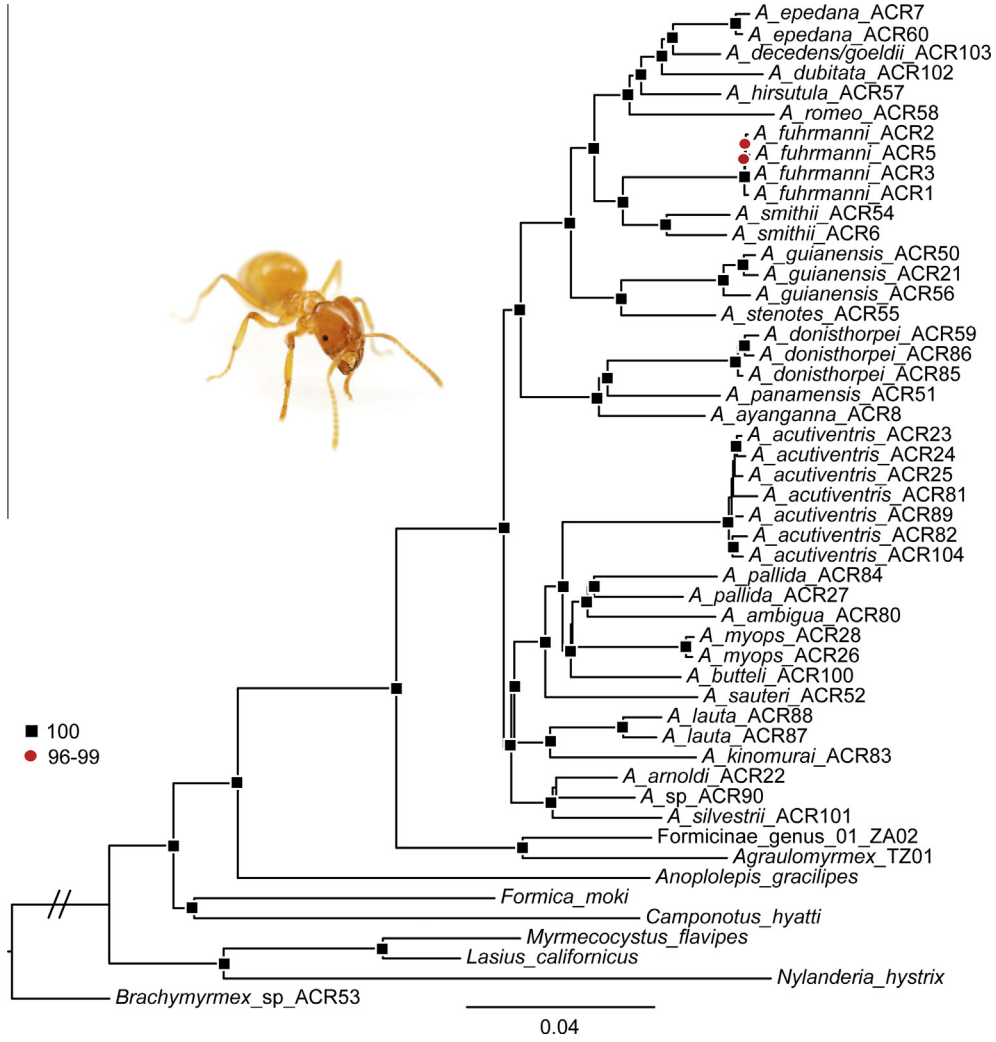

Fig. 2. Phylogeny of *Acropyga* ants. RAxML best tree estimated from the concatenated, partitioned UCE-944 data set, with support values from 100 RAxML bootstrap analyses mapped on the respective nodes. Black squares indicate 100% bootstrap support (BS), red circles indicate BS = 96–99; BS < 96 not shown. Scale bar depicts nucleotide substitution per site. The phylogeny is rooted with *Brachymyrmex*_sp_ACR53. *Acropyga* image courtesy of Alex Wild photography (www.alexanderwild.com). (For interpretation of the references to color in this figure legend, the reader is referred to the web version of this article.)

diversification in *Acropyga* appears to have occurred between ca. 8–20 Ma (Figs. 4 and S1). Age estimations based on BEAST analyses on the two random sets of 100 UCE loci were similar (<2 Ma difference) and confirmed the results presented above, although lower support values and some weakly-supported topological changes were recovered for one of these subsets. These additional results are detailed in Table S5 and Fig. S2.

3.4. Trait evolution

We found the 'equal rates' (ER) model to be best-fitting to both mandible and mealybug association in *Acropyga*, as logLikelihood values were not significantly worse than those estimated for the more complex SYM and ARD models (Table 3). We thus show ancestral states as reconstructed under the ER model (Fig. 5 and Table 4). Excluding versus including the 'hybrid' taxon *A. decedens/goeldii* did not have an effect on results. We reconstructed the possession of five mandibular teeth as the ancestral state in *Acropyga* (70% probability). The mealybug genus *Neochavesia* is suggested as ancestral mutualist partner of *Acropyga*, but with only slightly higher probability than the genus *Eumyrmococcus* (node 45, 0.46 vs 0.41, respectively; Tables 4 and S6). Throughout the evolution of Old World *Acropyga* (node 33, Fig. 5), associations with *Eumyrmococcus* and a mandibular structure with five teeth seem to have been retained, and present the most probable ancestral state for all species. In New World *Acrogyga* (node 44), our results show a reduction in mandibular teeth count in the lineage subtended by node 41 (Fig. 5), whereas the five-toothed state is retained in the lineage including *A. panamensis*, *A. donisthorpei* and *A. ayanganna* (node 43). The New World *Acropyga* further probably evolved in close association with mealybugs from the genus *Neochavesia*, until a more recent switch occurred to a mutualistic association with the genus *Rhizoecus*.

4. Discussion

4.1. Phylogenetic relationships of Acropyga ants

Both our concatenated and species tree analyses recovered a fully resolved and mostly highly supported phylogeny for *Acropyga* ants. On the species level these analyses estimated identical topologies (Figs. 2 and 3). Uncertainty is confined only to two nodes in the phylogeny with BS < 100, for which the BEAST topology (based on 100 UCE loci) also showed different results. Perhaps the most striking novel result in our study is the strong support for

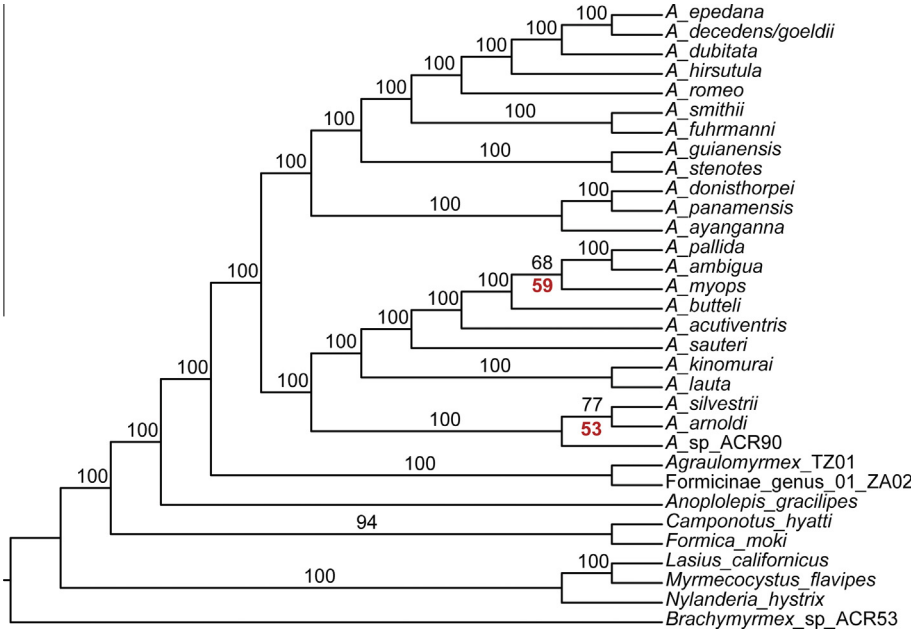

Fig. 3. *Acropyga* species tree. Bootstrapped species tree estimated with ASTRAL-II, after statistical weighted binning of the 944 UCE loci. The analysis required all taxa to be assigned to one respective species. Red colored support values indicate bootstrap support as estimated in the concatenated analysis (see Fig. 2). The tree is rooted with *Brachymyrmex*_sp_ACR53. (For interpretation of the references to color in this figure legend, the reader is referred to the web version of this article.)

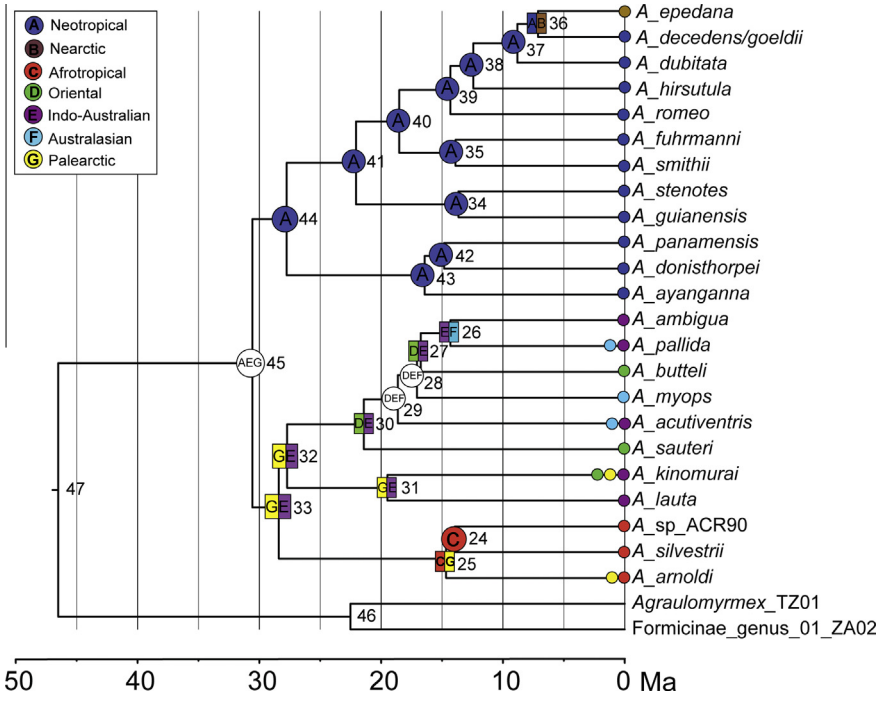

Fig. 4. Time-calibrated phylogeny depicting biogeographic history of *Acropyga*. Maximum clade credibility tree summarized from 55,793 trees as estimated with the UCE-100-best data set under a relaxed-clock model and three calibration priors (see Table 1). Node numbers refer to Tables 2 and S5. Ancestral ranges estimated by RASP under the S-DEC model are mapped onto respective nodes. A = Neotropical, B = Nearctic, C = Afrotropical, D = Oriental, E = Indo-Australian, F = Australasian, G = Palearctic. All but the two most closely related outgroup taxa were removed for BEAST analysis, and all outgroups were removed for biogeographic analysis.

a sister group relationship of separate New World and Old World *Acropyga* clades, which has not been recovered in previous analyses (LaPolla, 2004; LaPolla et al., 2006). Based on a morphological phylogeny of 25 *Acropyga* species LaPolla (2004), had already suggested a close association of all Neotropical taxa, but was not able to recover monophyly for these. Relationships of the Old World taxa further remained unresolved in this study (LaPolla, 2004), except for a suggested sister group relationship of *A. arnoldi* with the rest of *Acropyga* – although it is important to note that because that study was based largely on male genitalic structures *A. palearctica* and *A. silvestrii* (for which males were unknown at the time) were not included in the analysis. In contrast, our analyses found *A. arnoldi* to be part of a lineage sister to the remaining Old World species. Overall, our results broadly correspond with LaPolla's

Table 2
Results of dating analyses and ancestral range reconstructions. Posterior probabilities (PP), median ages, 95% HPD age intervals as estimated by BEAST on the UCE-100-best data set, as well as the most probable biogeographic range and its probability for each node of the phylogeny as reconstructed by RASP. Node numbers correspond to Fig. 4. A = Neotropical, B = Nearctic, C = Afrotropical, D = Oriental, E = Indo-Australian, F = Australasian, G = Palearctic.

Node	PP	Age - median	Age - 95%	Range	Range - PP
24	0.97	14.0	7.82, 21.0	C	100
25	1	14.7	8.48, 22.13	CG	63.3
26	0.97	14.3	8.26, 20.89	EF	59.6
27	0.63	16.8	10.3, 23.56	DE	49.5
28	0.97	17.1	10.77, 24.09	DEF	94.4
29	1	18.6	12.0, 26.01	DEF	69.9
30	1	21.4	14.27, 29.25	DE	53.7
31	1	19.5	10.29, 29.17	GE	64.4
32	1	27.7	19.6, 36.53	GE	58.1
33	1	28.4	20.36, 37.63	GE	57.5
34	0.97	13.7	7.9, 20.1	A	100
35	0.97	13.9	8.53, 19.83	A	100
36	0.99	7.1	3.91, 11.13	AB	99.7
37	1	8.8	5.2, 13.36	A	69.0
38	1	12.4	7.54, 18.13	A	99.7
39	0.98	14.3	9.39, 20.19	A	100
40	0.97	18.5	12.72, 25.07	A	100
41	1	22.1	14.68, 30.75	A	100
42	0.96	14.8	9.15, 21.86	A	100
43	1	16.4	9.65, 25.89	A	100
44	1	27.8	18.54, 38.81	A	100
45	1	30.6	21.52, 40.19	AEG	64
46	1	22.5	13.82, 32.38	n/a	n/a
47	1	46.5	36.25, 58.1	n/a	n/a

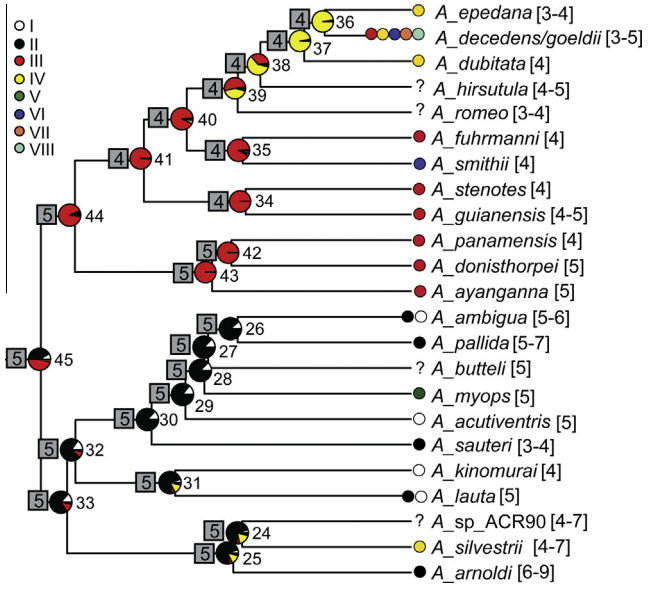

Fig. 5. Evolution of mandibular teeth and mealybug associations in *Acropyga*. Ancestral state reconstructions as estimated with *corHMM* under the ER model. The phylogeny is identical to the time-calibrated tree in Fig. 4. Pie charts represent ancestral reconstructions of mealybug associations, with the following color coding: I: *Xenococcus*, II: *Eumyrmococcus*, III: *Neochavesia*, IV: *Rhizoecus*, V: *Acropygorthezia*, VI: *Geococcus*, VII: *Capitisetella*, VIII: *Dysmicoccus*. Gray boxes give reconstructions of mandibular tooth count; terminal states are given in brackets after species name.

Table 3
Model fit for ancestral state reconstructions. Comparison of model fit for ancestral state reconstructions of xenococcine associations and number of mandibular teeth. ER: equal rates model, SYM: symmetric model, ARD: all rates different. LnL = LogLikelihood of model fit; Rates = number of rates in the model of evolution, p(chisqu) = the resulting p-value from a Chi-Square test comparing two respective models. Non-significant p-values are given in italics.

Mandibular teeth	ER	SYM	ARD
LnL	−20.998	−12.696	−12.216
Rates	1	21	42
p (chisqu(ER-SYM))		*0.999*	
p (chisqu(ER-ARD))			*0.679*
Xenococcines	**ER**	**SYM**	**ARD**
LnL	−30.252	−20.250	−19.043
Rates	1	28	56
p (chisqu(ER-SYM))		*0.831*	
p (chisqu(ER-ARD))			*1.000*

(2004) eight species-groups for the genus, but here we were able to significantly advance understanding of deeper level relationships. However, we observed little agreement of our phylogenomic analysis with the study on Papua New Guinean *Acropyga* by Janda et al. (2016), which included seven species that were also analyzed in our data set. For example, in our analyses *A. acutiventris* grouped as sister to the clade (*A. myops* (*A. butteli* (*A. pallida*, *A. ambigua*))) (see Figs. 2–4), whereas Janda et al. (2016) recovered *A. pallida* as sister to *A. acutiventris* (although with low support), and a clade containing *A. lauta* and *A. ambigua* was supported to be the sister clade of the two. Another disagreement between ours and their study is that Janda et al. (2016) estimated *A. arnoldi* to be sister to two New World species, *A. epedana* and *A. donisthorpei*, and not to be part of a lineage sister to all the remaining Old World taxa, as was recovered in our analyses. We attribute these differences to limited gene and taxon sampling in the Janda et al. (2016) analyses, as this study was based only on four gene fragments and very few non-Melanesian *Acropyga* species.

Table 4
Results of ancestral state reconstructions. Ancestral states reconstructed under the ER model, showing probabilities of the likeliest state for Xenococcine associations and number of mandibular teeth. Node numbers correspond to Figs. 4 and 5. Xenococcine associations: 2: *Eumyrmococcus*, 3: *Neochavesia*, 4: *Rhizoecus*.

Node	Xenococcine association		Mandibular teeth number	
	State	Prob.	State	Prob.
24	II	0.69	5	0.46
25	II	0.73	5	0.46
26	II	0.88	5	0.99
27	II	0.85	5	1.00
28	II	0.85	5	1.00
29	II	0.83	5	0.99
30	II	0.84	5	0.78
31	II	0.52	5	0.71
32	II	0.73	5	0.72
33	II	0.71	5	0.72
34	III	1.00	4	0.98
35	III	0.91	4	1.00
36	IV	0.97	4	1.00
37	IV	0.96	4	1.00
38	IV	0.60	4	1.00
39	III	0.51	4	1.00
40	III	0.92	4	1.00
41	III	0.97	4	0.97
42	III	1.00	5	0.80
43	III	1.00	5	0.80
44	III	0.92	5	0.67
45	III	0.46	5	0.70

4.2. Biogeographic history

Robust resolution of relationships between major *Acropyga* lineages, in combination with divergence age estimates, have shed substantial light on the biogeographic history of the genus. We estimated a crown-group age of 30 Ma for *Acropyga*, which corresponds well with an estimate for the group obtained in a larger

study on formicine ant evolution and biogeographic history (Blaimer et al., 2015), and is also consistent with the absence of the genus from Baltic amber. This Oligocene MRCA of *Acropyga* was reconstructed with a widespread Old World and New World distribution (Palearctic, Indo-Australian and Neotropical) in our analysis, followed by a subsequent divergence between Old World and New World *Acropyga* only a few million years later. Our knowledge of morphology and likely relationships of the remaining *Acropyga* species absent from our phylogeny also supports this early fundamental biogeographic split. We have sampled broadly across all biogeographic regions, and all of the species absent from the present investigation occupy ranges similar to their closest relatives – with the exception of *A. palearctica*, for which we included this complementary distribution in our analyses. Nonetheless, the rapid early diversification of *Acropyga* into two main biogeographic clades is somewhat surprising, given that previous studies considered *Acropyga* ants to be very poor dispersers based on its cryptobiotic lifestyle and suggested the genus may be of Gondwanan origin (LaPolla, 2004). However, this hypothesis predated most of our current knowledge on the timescale of ant evolution (Brady et al., 2006; Moreau and Bell, 2013; Moreau et al., 2006; Ward et al., 2015), and other examples of recently evolved ant genera that have succeeded in attaining widespread distributions have been revealed. For example, the hyperdiverse and globally distributed genus *Camponotus* may also be of a fairly recent Oligocene or Miocene origin (23–27 Ma Blaimer et al., 2015). The acrobat ants (genus *Crematogaster*) evolved in the Eocene, but most of their diversification and global dispersal also occurred in the Oligocene and Miocene (Blaimer, 2012). In contrast, *Polyrhachis*, the spiny ants, are of a similar age as *Crematogaster* (~40 Ma Mezger and Moreau, 2016), but never dispersed to the New World. In comparison with the small, soil-nesting *Acropyga* ants, however, all of the above genera represent species-rich and conspicuous groups of ants.

Janda et al. (2016) estimated a younger crown-group age for *Acropyga* at around 20 Ma. Beyond the aforementioned limitations in ingroup sampling, the younger estimate in their study may have been heavily influenced by a calibration on the root node, which is defined in their analysis as the split between the outgroup taxon *Anoplolepis* and *Acropyga*. The genus *Anoplolepis* was recovered as the sister to the remainder of the plagiolepidine clade in a larger analysis on the subfamily Formicinae, diverging from this clade (including *Acropyga*) ~74 Ma (Blaimer et al., 2015). This subfamily-wide analysis had not yet been available at the time their study was carried out, and Janda et al. (2016) calibrated the divergence of *Acropyga* with the former using a normal distribution with a mean of 45 Ma, which could plausibly explain their younger age estimates.

In a larger biogeographic study of the subfamily Formicinae, the clade Plagiolepidini, which *Acropyga* was found to be part of, has a predominantly Paleotropical distribution (Blaimer et al., 2015). Despite our inconclusive range reconstructions in the present study, we therefore suggest that ancestral *Acropyga*, too, may have evolved in the Old World tropics. Two alternative biogeographic scenarios could further explain the subsequent early split between the New World and Old World *Acropyga* clade and the current distribution of the genus. For one, a single dispersal event from the Old World to the New World between 28 and 30 Ma may have led to the present biogeographic distribution of the two main *Acropyga* lineages. Alternatively, it is possible that paleoclimatic changes have generated the distribution of the two main lineages without the need for long-distance dispersal. A warm-temperate climate prevailing in the Eocene throughout the Holarctic and Palearctic (Scotese, 2002) could have allowed one or several widespread ancestral *Acropyga* species to exist in these regions, where cold climate presently prevents the occurrence of the genus. Starting in the late Eocene and Oligocene, progressive climate cooling led to shrinking of warm-temperate and tropical habitats, which in turn possibly mediated vicariance of widespread ancestral representatives of *Acropyga*, thereby creating the present separation of lineages in the New World and Old World tropics. A similar scenario has been proposed for some groups of plants (Davis et al., 2002; Erkens et al., 2009), but would require an Eocene ancestor of *Acropyga* to migrate between the Palearctic and the Holarctic via a North Atlantic landbridge (McKenna, 1983).

Fossil evidence that could help to distinguish between either of these scenarios is sparse. The only known *Acropyga* fossil, *A. glaesaria*, occurs in 15–20 Ma old Dominican amber and would fit with either an early dispersal or a vicariant, ancestral presence of the genus in the New World. Morphologically, however, this fossil species presents a conundrum since it shows more similarities with the extant Old World *Acropyga* fauna (LaPolla, 2005), and could represent indeed an ancestral, once widespread lineage.

4.3. Evolution of Acropyga – root mealybug associations

Comparison of our *Acropyga* phylogeny with phylogenetic information from their xenococcine mealybug mutualists (Schneider and LaPolla, 2011) provides insights into the evolution of trophobiosis between these two groups. The morphological phylogeny from Schneider and LaPolla (2011) supported four major xenococcine groups, although relationships among these groups remained unresolved (Fig. 6). Intriguing patterns of relationships between the ants and mealybugs have emerged in our analyses, although a formal cospeciation analysis will need to await further study from both groups. For one, the biogeographic variation of this association is to date poorly studied, and this may have had an effect on results presented in our study. For many species only few records of associated mealybugs are available, thus estimates of fidelity of both partners are difficult. For species where many samples are available across a broad geographic range, however, remarkable fidelity of ant-mealybug associations has been found – for example, only two species of *Xenococcus* mealybugs live in association with *A. acutiventris* (LaPolla, 2004), a species that ranges from India, extending throughout insular southeast Asia and northern Australia. Thus, although our discussion of association patterns in the following must be viewed as somewhat preliminary, we intend to provide a first, basic framework for further analyses.

The early split of *Acropyga* into Old and New World clades is consistent with the recovery of a New World mealybug clade, *Neochavesia*, the only xenococcines associated with *Acropyga* in this bioregion (Fig. 6). Our analyses indicate that *Acropyga* in the New World almost certainly evolved tending *Neochavesia*, only to later switch to other rhizoecines such as *Rhizoecus* around 10–15 million years ago (Fig. 5). Outside of the Xenococcinae, *Acropyga* appear to

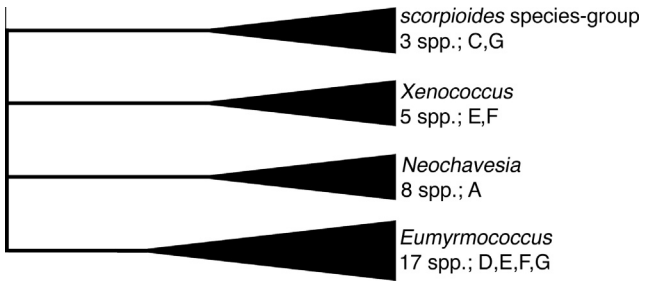

Fig. 6. Simplified xenococcine phylogeny. Summary of xenococcine morphological phylogeny following Schneider and LaPolla (2011) with modifications. Species numbers shown represent number of xenococcine species in each clade; A = Neotropical, B = Nearctic, C = Afrotropical, D = Oriental, E = Indo-Australian, F = Australasian, G = Palearctic.

most commonly enter into mutualistic relationships with *Rhizoecus* mealybugs. *Rhizoecus* is a large genus of root mealybugs (122 spp. listed on the Encyclopedia of Life website (www.eol.org), including the likely synonym *Ripersiella* (Hodgson, 2012)) and the species associated with *Acropyga* need further study. Association with *Rhizoecus* occurs in several New World *Acropyga* species (*A. decedens*, *A. epedana*, *A. exsanguis*, *A. goeldii*, and *A. dubitata*), and in one species, *A. epedana*, trophophoresy has also been observed (Smith et al., 2007; Williams and LaPolla, 2004). There is also at least one association with *Rhizoecus* in the Old World, with an *A. silvestrii* nest found with an undescribed *Rhizoecus* species in Tanzania (Fig. 5).

Clearly there have been some major switches in symbiont partners by *Acropyga*, perhaps best exemplified by *A. myops*. This species is associated with *Acropygorthezia williamsi*, the only non-Rhizoecidae utilized by *Acropyga*. The switch to an entirely different family of scale insects (Ortheziidae) is also interesting because *Acropygorthezia williamsi* show a number of novel morphological adaptations compared to all other ortheziids, that are almost certainly adaptations for living with *Acropyga* ants (LaPolla et al., 2008). However, it is important to note that while several *Acropyga* species have been reported as associated with more than one xenococcine species, sometimes even belonging to different genera (Fig. 5), no individual *Acropyga* nest to date has ever been found with more than one mealybugs species inside.

Eurmyrmococcus mealybugs were not recovered as monophyletic by Schneider and LaPolla (2011), with the *scorpioides* species-group falling outside of the genus (Fig. 6). Interestingly, this group of species is associated with *A. arnoldi* (and *A. paleartica*, which was not included in this study as noted above, but is likely the sister to *A. arnoldi*) (nodes 24 & 25; Fig. 5), which belongs to the Afrotropical/western Palearctic clade. Within the remainder of the Old World clade, no clear pattern is evident on lineage-specific associations of *Acropyga* and mealybugs (Fig. 5). Reconstruction of the mealybug group at the origin of this association (the base of *Acropyga*) also remains equivocal, with nearly the same probability for either *Eumyrmococcus* or *Neochavesia*.

The diversity of mandibular forms found in *Acropyga* (Fig. 1) seems likely be a product of its close association with scale insects, although how this affects their trophobiotic relationship is unclear at this time. Our results indicate that five mandibular teeth were the ancestral condition for *Acropyga*, and this is largely retained in Old World species. But beyond tooth number, the shape of the mandible and the size of teeth can change rather dramatically (Fig. 1). So, while many Old World species retain a broad mandible, there is a trend among New World species for not only reduction in teeth number, but also for the mandible to become thinner, with a large space forming between the inner mandibular margin and the anterior clypeal margin (e.g., Fig. 1E). This is also accompanied by a lengthening of the mandibular teeth, most notably the apical tooth. The Old World *butteli* species-group is notable because species in this clade have a large, rectangular basal tooth. This same basal tooth character state is seen convergently in *A. panamensis* and in *A. tricuspis* (although in this species, the basal tooth has three distinct cuspids associated with it) in the New World. The sole fossil *Acropyga* species known (*A. glaesaria*, from New World Dominican amber) does not shed more light on mandibular evolution in *Acropyga*. On the contrary the queens were found to have eight teeth, a much higher number than seen in any extant New World *Acropyga*. However, only four fossil queens were available for examination and the mandibles were not fully visible in all of these. Thus it remains possible that this fossil species showed more variation in tooth count (as for example seen in the extant *A. arnoldi* and *A. silvestrii*) than was observed. In any case, our results call for a closer examination of a possible correlation between mandible variation and mealybug partners in *Acropyga*.

4.4. Conclusions

Our phylogenomic UCE data robustly resolved the species-level phylogeny for *Acropyga* ants. We observed virtually no differences in phylogenetic inference between our concatenated analysis and the species-tree approach, suggesting absence of conflict between gene trees. We found strong evidence for a fundamental Old World – New World split in *Acropyga* and independent diversification of these two main lineages since the late Oligocene (after ~28 Ma). The origin of *Acropyga* remained uncertain in our biogeographic analysis, but an Old World ancestor for *Acropyga* may be likely given the close phylogenetic relationship of the genus with exclusively Paleotropical taxa in the tribe Plagiolepidini.

Although our study goes some way toward establishing broad patterns of *Acropyga*/mealybug associations, it also highlights the need for additional field studies and targeted collections of the ants in association with their mealybugs, data required to fully assess the patterns that have started to emerge here. Mealybug associations in some *Acropyga* species are currently based on very few collections, while mutualist information for other species is completely lacking. Our results also suggest that another fruitful direction for research is the functional morphology of *Acropyga* mandibular variation as it relates to mealybug associations. These additional biological data could in turn inform detailed phylogenies of both partners, which would be required for stringent tests of codiversification. Here, we demonstrate that UCE data provide a robust phylogenomic source for the ants, and similar types of data could also be applied to the mealybugs in the future.

Acknowledgements

This study was supported by NSF Grant DEB-0743542 (to JSL and SGB) and the Smithsonian Institution Competitive Grants Program for Science (to SGB). BBB and MGB were partly supported by a Peter Buck Postdoctoral Fellowship and MGB was partly supported by NSF Grant DEB-1354739. We are grateful to A. Jesovnik and J. Sosa-Calvo for help with laboratory procedures. All of the laboratory and the computer work were conducted in and with the support of the L.A.B. facilities of the National Museum of Natural History. We thank two anonymous reviewers for helpful comments on the manuscript. The following individuals kindly provided us specimens for use in this work: G. Alpert, C. Burwell, J. Delabie, D. General, M. Janda, F. Kozar, J. Longino, E. Sarnat, T. Schultz, C. Smith, and A. Wild. Images reproduced in Fig. 1 are courtesy of AntWeb (www.antweb.org) and photographers S. Hartman, W. Ericson, E. Ortega, A. Nobile and J. Sosa-Calvo; the ant image incorporated in Fig. 2 is courtesy of Alex Wild photography (www.alexanderwild.com).

Appendix A. Supplementary material

Supplementary data associated with this article can be found, in the online version, at http://dx.doi.org/10.1016/j.ympev.2016.05.030.

References

Bayzid, M.S., Mirarab, S., Boussau, B., Warnow, T., 2015. Weighted statistical binning: enabling statistically consistent genome-scale phylogenetic analyses. PLoS One 10, e0129183.

Beaulieu, J.M., Tank, D.C., Donoghue, M.J., 2013. A Southern Hemisphere origin for campanulid angiosperms, with traces of the break-up of Gondwana. BMC Evol. Biol. 13, 80.

Blaimer, B.B., Brady, S.G., Schultz, T.R., Lloyd, M.W., Fisher, B.L., Ward, P.S., 2015. Phylogenomic methods outperform traditional multi-locus approaches in resolving deep evolutionary history: a case study of formicine ants. BMC Evol. Biol. 15, 271.

Blaimer, B.B., 2012. Acrobat ants go global – Origin, evolution and systematics of the genus *Crematogaster* (Hymenoptera: Formicidae). Mol. Phylogenet. Evol. 65, 421–436.
Blumenstiel, B., Cibulskis, K., Fisher, S., DeFelice, M., Barry, A., Fennell, T., Abreu, J., Minie, B., Costello, M., Young, G., 2010. Targeted exon sequencing by in-solution hybrid selection. Curr. Prot. Hum. Gen. (Suppl 66), 1–8 (Unit 18.4).
Bolger, A.M., Lohse, M., Usadel, B., 2014. Trimmomatic: a flexible trimmer for Illumina sequence data. Bioinformatics, btu170:1–7.
Bolton, B., 1995. A taxonomic and zoogeographical census of the extant ant taxa (Hymenoptera: Formicidae). J. Nat. Hist. 29, 1037–1056.
Bolton, B., 2000. The ant tribe Dacetini. Mem. Am. Entomol. Inst. 65, 1–1028.
Brady, S.G., Schultz, T.R., Fisher, B.L., Ward, P.S., 2006. Evaluating alternative hypotheses for the early evolution and diversification of ants. Proc. Natl. Acad. Sci. USA 103, 18172–18177.
Brown, W., 1945. An unusual behavior pattern observed in a Szechuanese ant. J. W. China Border Res. Soc. 15, 185–186.
Bünzli, G.H., 1935. Untersuchungen über coccidophile Ameisen aus den Kaffeefeldern von Surinam. Mitt. Schweiz. Entomol. Ges. 16, 455–593.
Buschinger, A., Heinze, J., Jessen, K., Douwes, P., Winter, U., 1987. First European record of a queen ant carrying a mealybug during her mating flight. Naturwissenschaften 74, 139–140.
Castresana, J., 2000. Selection of conserved blocks from multiple alignments for their use in phylogenetic analysis. Mol. Biol. Evol. 17, 540–552.
Crawford, N.G., Parham, J.F., Sellas, A.B., Faircloth, B.C., Glenn, T.C., Papenfuss, T.J., Henderson, J.B., Hansen, M.H., Simison, W.B., 2015. A phylogenomic analysis of turtles. Mol. Phylogenet. Evol. 83, 250–257.
Davis, C.C., Bell, C.D., Mathews, S., Donoghue, M.J., 2002. Laurasian migration explains Gondwanan disjunctions: evidence from Malpighiaceae. Proc. Natl. Acad. Sci. USA 99, 6833–6837.
Degnan, P.H., Lazarus, A.B., Brock, C.D., Wernegreen, J.J., 2004. Host-symbiont stability and fast evolutionary rates in an ant-bacterium association: Cospeciation of *Camponotus* species and their endosymbionts, *Candidatus Blochmannia*. Syst. Biol. 53, 95–110.
Drummond, A.J., Suchard, M.A., Xie, D., Rambaut, A., 2012. Bayesian phylogenetics with BEAUti and the BEAST 1.7. Mol. Biol. Evol. 29, 1969–1973.
Eberhard, W., 1978. Mating swarms of a South American *Acropygia* (Hymenoptera: Formicidae). Entomol. News 89, 14–16.
Economo, E.P., Sarnat, E.M., Janda, M., Clouse, R., Klimov, P.B., Fischer, G., Blanchard, B.D., Ramirez, L.N., Andersen, A.N., Berman, M., Guénard, B., Lucky, A., Rabeling, C., Wilson, E.O., Knowles, L.L., 2015. Breaking out of biogeographical modules: range expansion and taxon cycles in the hyperdiverse ant genus *Pheidole*. J. Biogeogr. 42, 2289–2301.
Erkens, R.H., Maas, J., Couvreur, T.L., 2009. From Africa via Europe to South America: migrational route of a species-rich genus of Neotropical lowland rain forest trees (*Guatteria*, Annonaceae). J. Biogeogr. 36, 2338–2352.
Faircloth, B., 2013. Illumiprocessor: a trimmomatic wrapper for parallel adapter and quality trimming, http://dx.doi.org/10.6079/J9ILL.
Faircloth, B.C., 2016. PHYLUCE is a software package for the analysis of conserved genomic loci. Bioinformatics 32, 786–788.
Faircloth, B.C., Branstetter, M.G., White, N.D., Brady, S.G., 2015. Target enrichment of ultraconserved elements from arthropods provides a genomic perspective on relationships among Hymenoptera. Mol. Ecol. Res. 15, 489–501.
Faircloth, B.C., McCormack, J.E., Crawford, N.G., Harvey, M.G., Brumfield, R.T., Glenn, T.C., 2012. Ultraconserved elements anchor thousands of genetic markers spanning multiple evolutionary timescales. Syst. Biol. 61, 717–726.
Federman, S., Dornburg, A., Downie, A., Richard, A.F., Daly, D.C., Donoghue, M.J., 2015. The biogeographic origin of a radiation of trees in Madagascar: implications for the assembly of a tropical forest biome. BMC Evol. Biol. 15, 216.
Frandsen, P.B., Calcott, B., Mayer, C., Lanfear, R., 2015. Automatic selection of partitioning schemes for phylogenetic analyses using iterative k-means clustering of site rates. BMC Evol. Biol. 15, 13.
Grabherr, M.G., Haas, B.J., Yassour, M., Levin, J.Z., Thompson, D.A., Amit, I., Adiconis, X., Fan, L., Raychowdhury, R., Zeng, Q., Chen, Z., Mauceli, E., Hacohen, N., Gnirke, A., Rhind, N., di Palma, F., Birren, B.W., Nusbaum, C., Lindblad-Toh, K., Friedman, N., Regev, A., 2011. Full-length transcriptome assembly from RNA-Seq data without a reference genome. Nat. Biotechnol. 29, 644–652.
Hodgson, C., 2012. Comparison of the morphology of the adult males of the rhizoecine, phenacoccine and pseudococcine mealybugs (Hemiptera: Sternorrhyncha: Coccoidea), with the recognition of the family Rhizoecidae Williams. Zootaxa 3291, 1–79.
Hölldobler, B., Wilson, E.O., 2011. The Leafcutter Ants: Civilization by Instinct. W.W. Norton & Company, Inc..
Ivens, A.B.F., 2015. Cooperation and conflict in ant (Hymenoptera: Formicidae) farming mutualisms – a review. Myrmecol. News 21, 19–36.
Janda, M., Matos-Maraví, P., Borovanska, M., Zima Jr., J., Youngerman, E., Pierce, N.E., 2016. Phylogeny and population structure of the ant genus *Acropyga* (Hymenoptera: Formicidae) in Papua New Guinea. Invertebr. Syst. 30, 28–40.
Katoh, K., Asimenos, G., Toh, H., 2009. Multiple alignment of DNA sequences with MAFFT. In: Bioinformatics for DNA Sequence Analysis. Springer, pp. 39–64.
Kikuchi, Y., Hosokawa, T., Nikoh, N., Meng, X.-Y., Kamagata, Y., Fukatsu, T., 2009. Host-symbiont co-speciation and reductive genome evolution in gut symbiotic bacteria of acanthosomatid stinkbugs. BMC Biol. 7, 2.
LaPolla, J., 2004. *Acropyga* (Hymenoptera: Formicidae) of the world. Contrib. Am. Entomol. Inst. 33, 1–130.
LaPolla, J., Spearman, L., 2007. Characterization of an *Acropyga arnoldi* mating swarm and early stage colony founding behavior. Trans. Am. Entomol. Soc. 133, 449–452.
LaPolla, J.S., 2005. Ancient trophophoresy: a fossil *Acropyga* (Hymenoptera: Formicidae) from Dominican amber. Trans. Am. Entomol. Soc. 131, 21–28.
LaPolla, J.S., 2006. Description of the male of *Acropyga paleartica* Menozzi. Myrmecolog. Nachr. 8, 171–173.
LaPolla, J.S., Burwell, C., Brady, S.G., Miller, D.R., 2008. A new ortheziid (Hemiptera: Coccoidea) from Australia associated with *Acropyga myops* Forel (Hymenoptera: Formicidae) and a key to Australian Ortheziidae. Zootaxa 1946, 55–68.
LaPolla, J.S., Cover, S.P., Mueller, U.G., 2002. Natural history of the mealybug-tending ant, *Acropyga epedana*, with descriptions of the male and queen castes. Trans. Am. Entomol. Soc. 128, 367–376.
LaPolla, J.S., Schultz, T.R., Kjer, K.M., Bischoff, J.F., 2006. Phylogenetic position of the ant genus *Acropyga* Roger (Hymenoptera: Formicidae) and the evolution of trophophoresy. Insect Syst. Evol. 37, 197–212.
McKenna, M.C., 1983. Cenozoic Paleogeography of North Atlantic Land Bridges. Structure and Development of the Greenland-Scotland Ridge. Springer, pp. 351–399.
Mehdiabadi, N.J., Schultz, T.R., 2010. Natural history and phylogeny of the fungus-farming ants (Hymenoptera: Formicidae: Myrmicinae: Attini). Myrmecol. News 13, 37–55.
Mezger, D., Moreau, C.S., 2016. Out of South-East Asia: phylogeny and biogeography of the spiny ant genus *Polyrhachis* Smith (Hymenoptera: Formicidae). Syst. Ent. 41, 369–378.
Mirarab, S., Warnow, T., 2015. ASTRAL-II: coalescent-based species tree estimation with many hundreds of taxa and thousands of genes. Bioinformatics 31, i44–i52.
Moreau, C.S., Bell, C.D., 2013. Testing the museum versus cradle tropical biological diversity hypothesis: phylogeny, diversification, and ancestral biogeographic range evolution of the ants. Evolution 67, 2240–2257.
Moreau, C.S., Bell, C.D., Vila, R., Archibald, S.B., Pierce, N.E., 2006. Phylogeny of the ants: diversification in the age of angiosperms. Science 312, 101–104.
Prins, A., 1982. Review of Anoplolepis with reference to male genitalia, and notes on Acropyga (Hymenoptera, Formicidae). Ann. S. Afr. Mus. 89 (Part 3), 247.
Schneider, S.A., LaPolla, J.S., 2011. Systematics of the mealybug tribe Xenococcini (Hemiptera: Coccoidea: Pseudococcidae), with a discussion of trophobiotic associations with *Acropyga* Roger ants. Syst. Ent. 36, 57–82.
Scotese, C.R., 2002. PALEOMAP. <www.scotese.com> (accessed 26.01.16).
Seo, T.-K., 2008. Calculating bootstrap probabilities of phylogeny using multilocus sequence data. Mol. Biol. Evol. 25, 960–971.
Shingleton, A.W., Stern, D.L., Foster, W.A., 2005. The origin of a mutualism: a morphological trait promoting the evolution of ant-aphid mutualisms. Evolution 59, 921–926.
Smith, B.T., Harvey, M.G., Faircloth, B.C., Glenn, T.C., Brumfield, R.T., 2013. Target capture and massively parallelsequencing of ultraconserved elements for comparative studies at shallow evolutionary time scales. Syst. Biol. 63, 83–95.
Smith, B.T., McCormack, J.E., Cuervo, A.M., Hickerson, M.J., Aleixo, A., Cadena, C.D., Perez-Eman, J., Burney, C.W., Xie, X., Harvey, M.G., Faircloth, B.C., Glenn, T.C., Derryberry, E.P., Prejean, J., Fields, S., Brumfield, R.T., 2014. The drivers of tropical speciation. Nature 515, 406–409.
Smith, C.R., Oettler, J., Kay, A., Deans, C., 2007. First recorded mating flight of the hypogeic ant, *Acropyga epedana*, with its obligate mutualist mealybug, *Rhizoecus colombiensis*. J. Insect Sci. 7 11.
Stamatakis, A., 2006. RAxML-VI-HPC: maximum likelihood-based phylogenetic analyses with thousands of taxa and mixed models. Bioinformatics 22, 2688–2690.
Taylor, R.W., 1992. Nomenclature and distribution of some Australian and New Guinean ants of the subfamily Formicinae (Hymenoptera: Formicidae). J. Aust. Entomol. Soc. 31, 57–69.
Terayama, M., 1988. Some taxonomical and biological notes on the myrmecophilous mealybug genus *Eumyrmococcus* (Homoptera: Pseudococcidae). Rostria 39, 643–648.
Ward, P.S., Brady, S.G., Fisher, B.L., Schultz, T.R., 2015. The evolution of myrmicine ants: phylogeny and biogeography of a hyperdiverse ant clade (Hymenoptera: Formicidae). Syst. Ent. 40, 61–81.
Weber, N.A., 1944. The Neotropical coccid-tending ants of the genus *Acropyga* Roger. Ann. Entomol. Soc. Am. 37, 89–122.
Williams, D., LaPolla, J., 2004. The subterranean mealybug, *Rhizoecus colombiensis* (Hambleton) (Hem., Pseudococcidae), described originally from Colombia, now found associated with the ant *Acropyga epedana* Snelling (Hym., Formicidae) in Arizona, USA. Entomologist's Monthly Magazine, vol. 140, p. 106.
Williams, D.J., 1998. Mealybugs of the genera *Eumyrmococcus* Silvestri and *Xenococcus* Silvestri associated with the ant genus *Acropyga* Roger and a review of the subfamily Rhizoecinae (Hemiptera, Coccoidea, Pseudococcidae). Bull. Br. Mus. Nat. Hist. (Ent.) 67, 1–64.
Yu, Y., Harris, A.J., Blair, C., He, X., 2015. RASP (Reconstruct Ancestral State in Phylogenies): a tool for historical biogeography. Mol. Phylogenet. Evol. 87, 46–49.

Supplementary laboratory and bioinformatics protocols

Molecular data collection

DNA was extracted destructively or non-destructively (specimen retained after extraction) from worker ants or pupae using a DNeasy Blood and TissueKit (Qiagen, Valencia, CA, USA). We quantified DNA for each sample using a Qubit fluorometer (High sensitivity kit, Life Technologies, Inc.) and sheared 1.8–245 ng (91 ng mean) DNA to a target size of approximately 500–600 bp by sonication (Q800, Qsonica LLC.). The sheared DNA was used as input for a modified genomic DNA library preparation protocol (Kapa Hyper Prep Library Kit, Kapa Biosystems) that incorporated "with-bead" cleanup steps (Fisher et al. 2011) and a generic SPRI substitute (Rohland and Reich 2012, "speedbeads" hereafter), as described by (Faircloth et al. 2015). We used TruSeq-style adapters during adapter ligation (Faircloth and Glenn 2012), and PCR amplified 50% of the resulting library volume (15 µL) using a reaction mix of 25 µL HiFi HotStart polymerase (Kapa Biosystems), 2.5 µL each of Illumina TruSeq-style i5 and i7 primers (5 µM each) and 5 µL double-distilled water (ddH20). We used the following thermal protocol: 98 ºC for 45 s; 13 cycles of 98 ºC for 15 s, 65 ºC for 30 s, 72 ºC for 60 s, and final extension at 72 ºC for 5 m. After rehydrating (in 23µL pH 8 Elution Buffer (EB hereafter)) and purifying reactions using 1.0X speedbeads, we combined groups of eight libraries at equimolar ratios into enrichment pools having final concentrations of 74–156 ng/µL.

We enriched each pool using a set of 2749 custom-designed probes (MYcroarray, Inc.) targeting 1510 UCE loci in Hymenoptera (see Faircloth et al. 2015). We followed library enrichment procedures for the MYcroarray MYBaits kit (Blumenstiel et al. 2010), except we

used a 0.1X concentration of the standard MYBaits concentration, and added 0.7 µL of 500 µM custom blocking oligos designed against our custom sequence tags. We ran the hybridization reaction for 24 h at 65 °C, subsequently bound all pools to streptavidin beads (MyOne C1; Life Technologies), and washed bound libraries according to a standard target enrichment protocol (Blumenstiel et al. 2010). We used the with-bead approach for PCR recovery of enriched libraries as described in Faircloth et al. (Faircloth et al. 2015). We combined 15 µL of streptavidin bead-bound, enriched library with 25 µL HiFi HotStart Taq (Kapa Biosystems), 5 µL of Illumina TruSeq primer mix (5 µM each) and 5 µL of ddH2O. We ran post-enrichment PCR using the following thermal profile: 98 °C for 45 s; 18 cycles of 98 °C for 15 s, 60 °C for 30 s, 72 °C for 60 s; and a final extension of 72 °C for 5 m. We purified resulting reactions using 1.0X speedbeads, and we rehydrated the enriched pools in 22 µL EB. We quantified 2 µL of each enriched pool using a Qubit fluorometer (broad range kit).

Enrichment was verified by amplifying seven UCE loci (for primers see Faircloth et al. 2015) targeted by the probe set. We set up a relative qPCR by amplifying two replicates of 1 ng of enriched DNA from each library at all seven loci and comparing those results to two replicates of 1 ng unenriched DNA for each library at all seven loci. We quantified post-enrichment library concentration with qPCR using a SYBR® FAST qPCR kit (Kapa Biosystems) on a ViiA™ 7 (Life Technologies). Following data collection, we computed the average of the replicate crossing point (C_p) values for each library at each amplicon, and we computed fold-enrichment values, assuming an efficiency of 1.78 and using the formula $1.78^{abs(\text{enriched } C_p - \text{unenriched } C_p)}$. We then created serial dilutions of each pool (1:200,000, 1:800,000, 1:1.000,000, 1:10.000,000) and performed qPCR library quantification, assuming an average library fragment length of 600 bp. Based on the size-adjusted concentrations estimated by qPCR, we pooled

libraries at equimolar concentrations and size-selected for 250–800 with a BluePippin (SageScience). The pooled libraries were sequenced using two partial lanes (both lanes included samples from other projects) of a 150-bp paired-end Illumina HiSeq 2500 run (U Cornell Genomics Facility). All of the laboratory work was conducted in and with support of the Laboratories of Analytical Biology (L.A.B.) facilities of the National Museum of Natural History. Quality-trimmed sequence reads generated as part of this study are available under submission SRP069792 from the NCBI Sequence Read Archive (http://www.ncbi.nlm.nih.gov/sra/SRP069792).

Processing and alignment of UCE data

We trimmed the demultiplexed FASTQ data output for adapter contamination and low-quality bases using Illumiprocessor (Faircloth, 2013: http://dx.doi.org/10.6079/J9ILL), based on the package Trimmomatic (Bolger et al. 2014). All further data processing described in the following relied on scripts within the PHYLUCE package (Faircloth et al. (in press); but see also (Faircloth et al. 2012)). We computed summary statistics on the data using the *get_fastq_stats.py* script, and assembled the cleaned reads using the *assemblo_trinity.py* wrapper around the program Trinity (version trinityrnaseq_r20140717) (Grabherr et al. 2011). Average sequencing coverage across assembled contigs was calculated using *get_trinity_coverage.py*.

To identify assembled contigs representing enriched UCE loci from each species, species-specific contig assemblies were aligned to a FASTA file of all enrichment baits using *match_contigs_to_probes.py*. (min_coverage=50, min_identity=80), and sequence coverage statistics (avg, min, max) for contigs containing UCE loci were calculated using *get_trinity_coverage_for_uce_loci.py*. Subsequently, we used *get_match_counts.py* to query the

relational database containing matched probes created in the previous step, in order to generate a list of UCE loci shared across all taxa. This list of UCE loci was then used in the *get_fastas_from_match_counts.py* script to create FASTA files for each UCE locus, which contain sequence data for taxa present at that particular locus. We aligned all data in all these FASTA files using MAFFT (Katoh et al. 2009) through *seqcap_align_2.py* (min-length=20, no-trim). Following alignment, we further trimmed our alignments using a wrapper script (*get_gblocks_trimmed_alignment_from _untrimmed.py*) for Gblocks (Castresana 2000) using the following settings: b1=0.5, b2=0.5, b3=12, b4=7. We selected a subset of UCE alignments for further analyses that had 70% taxon completeness for each locus ($\geq$ 35 of 50 taxa), using *get_only_loci_with_min_taxa.py* and thus retaining 944 UCE loci. We added missing data designators to each file with *add_missing_data_designators.py*, and generated alignment statistics across all alignments using *get_align_summary_data.py*. Finally, we concatenated individual alignments of UCE loci for each subset into one nexus alignment file with *format_nexus_files_for_raxml.py* for subsequent phylogenetic analyses.

Table S1: Collection data for *Acropyga* specimens sequenced in this study. Table listing unique identifiers of voucher specimens (deposited at USNM), collector and collection date, and locality information including elevation and GPS coordinates (in decimal degrees) where available.

Acropyga species	Voucher specimen	Collector	Collection Date	Country	Locality	Elevation (m)	Lat(DD)	Long(DD)
acutiventris	USNMENT01118000	S.G. Brady	Aug-2006	Australia	7km NE Lockerbie	90	-10.7570	142.5101
acutiventris	USNMENT01118001	S.G. Brady	Aug-2006	Australia	2km S Cape York	30	-10.7098	142.5292
acutiventris	USNMENT01118002	S.G. Brady	15-Aug-2006	Australia	1.6 km WSW Cape Tribulation	40	-16.0823	145.4615
acutiventris	USNMENT01118003	M. Janda	N/A	Papua New Guinea	Madang Prov; Ohu Village	100-200	-5.2667	145.6833
acutiventris	USNMENT01118004	J.S. LaPolla	24-Jun-2012	Cambodia	Koh Kong Prov; Cardamom Mtns.	475	11.8855	103.0756
acutiventris	USNMENT01118005	E.M. Sarnat	06-Feb-2008	Solomon Islands	Makira, 13.9 km SSW KiraKira	N/A	-10.5668	161.8915
acutiventris	USNMENT01118006	J.B. Wright	24-Jun-2012	Cambodia	Koh Kong Prov; Cardamom Mtns.	475	11.8855	103.0756
ambigua	USNMENT01118007	M. Janda	20-Feb-2004	Papua New Guinea	Madang, Baitabag Village	50	-5.1333	145.7833
arnoldi	USNMENT01118008	J.S. LaPolla	03-May-2006	South Africa	Cederberg Wilderness Area	998	-32.3416	19.0201
ayanganna	USNMENT01118009	J.S. LaPolla	12-Oct-2002	Guyana	Falls Camp	1134	5.3722	-59.9594
butteli	USNMENT01118030	J.S. LaPolla	29-Jun-2012	Cambodia	Koh Kong Prov; Cardamom Mtns.	475	11.8855	103.0756
decedens/goeldii	USNMENT01118010	T.R. Schultz	03-Aug-2012	Peru	Madre de Dios: Tambopata Prov.: Sachavacayoc Centre	193	-12.8532	-69.3674
donisthorpei	USNMENT01118011	J.S. LaPolla	27-Sep-2002	Guyana	Calm Water Creek; nr. Bartica	N/A	6.4677	-58.6193
donisthorpei	USNMENT01118012	J.R.M. Santos et al.	Nov-2007	Brazil	Ilheus, CEPAC	N/A	N/A	N/A
donisthorpei	USNMENT01118013	J.S. LaPolla	24-Aug-2007	Guyana	Iwokrama Forest Field Station	107	4.6758	-58.6845
dubitata	USNMENT01118014	J.S. LaPolla	31-Jul-2009	Dominican Republic	San Francisco Mtns; Loma Quita Espuela Reserve	290	19.3386	-70.1482
epedana	USNMENT01118015	J.S. LaPolla	Aug-2001	USA	AZ, Southwestern Research Station	1676	31.8887	-109.2080
epedana	USNMENT01118016	C.R. Smith	29-Jul-2005	USA	AZ, Southwestern Research Station	N/A	31.8838	-109.2063
fuhrmanni	USNMENT01118017	M. Velez	22-Oct-2003	Colombia	Quimbaya, Finca Santa Helena	1340	5.9667	-75.7167
fuhrmanni	USNMENT01118018	M. Velez	03-Feb-2004	Colombia	Chinchina (Caldas) Cenifcafe	1310	5.0167	-75.6000
fuhrmanni	USNMENT01118019	M. Velez	03-Feb-2004	Colombia	Chinchina (Caldas) Cenifcafe	1310	5.0167	-75.6000
fuhrmanni	USNMENT01118020	M. Velez	03-Feb-2004	Colombia	Chinchina (Caldas) Cenifcafe	1310	5.0167	-75.6000
guianensis	USNMENT01118021	J.S. LaPolla	06-Aug-2005	French Guiana	Nouragues Field Station	N/A	4.0833	-52.6833
guianensis	USNMENT01118022	T. Schultz, J. Sosa-Calvo, C. Marshall	02-Oct-2004	Peru	Madre de Dios: Los Amigos Field Station	274	-12.5690	-70.1009
guianensis	USNMENT01118023	J.S. LaPolla	07-Oct-2002	Guyana	Mt. Ayanganna Base Camp	732	5.3344	-59.9248
hirsutula	USNMENT01118024	A.L. Wild	11-Dec-2003	Ecuador	Napo; Carlos J. Arosemena Tola	500	-1.1500	-77.8833

Acropyga species	Voucher specimen	Collector	Collection Date	Country	Locality	Elevation (m)	Lat(DD)	Long(DD)
kinomurai	USNMENT01118025	N/A	17-Apr-2004	Philippines	Panicuason, Naga City	N/A	N/A	N/A
lauta	USNMENT01118026	E.M. Sarnat	21-Jan-2008	Fiji	Viti Levu, Colo-i-Suva Forest Park	186	-18.0666	178.4433
lauta	USNMENT01118027	E.M. Sarnat	06-Feb-2006	Solomon Islands	13.9 km SSW Kirakira, b/w Marone & Hauta Villages	825	-10.5668	161.8920
myops	USNMENT01118028	C. Burwell	Aug-2006	Australia	Bulimba Creek, Carindane suburb	N/A	-27.5008	153.1091
myops	USNMENT01118029	C. Burwell	Aug-2006	Australia	Bushland Reserve, Chelsea Road	N/A	-27.4837	153.1817
pallida	USNMENT01118031	C. Burwell	Aug-2006	Australia	vic. Ransome	N/A	-27.4914	153.1857
pallida	USNMENT01118032	N/A	20-Jun-2004	Philippines	Panicuason, Naga City	N/A	N/A	N/A
panamensis	USNMENT01118033	J. Sosa-Calvo	22-Oct-2006	Guyana	nr. Kamoa River, nr Kamoa R. Camp	394	1.5464	-58.8322
romeo	USNMENT01118034	J.S. LaPolla	09-Oct-2002	Guyana	Mt. Ayanganna Base Camp	752	4.7856	-59.2880
sauteri	USNMENT01118035	N/A	13-Jun-2002	Japan	Okinawa Is.; Sashiki Town	N/A	N/A	N/A
(new) sp.	USNMENT01118036	T. Pocs	19-Oct-1971	Tanzania	Ulu Guru Mountains	1700	N/A	N/A
silvestrii	USNMENT01118037	J.S. LaPolla	26-Mar-2011	Tanzania	Udzungwa Mountains	N/A	-8.0677	37.1259
smithii	USNMENT01118038	M. Velez	03-Feb-2004	Colombia	Chinchina (Caldas) Cenifcafe	1310	5.0167	-75.6000
smithii	USNMENT01118039	J.S. LaPolla	26-Sep-2004	Peru	Kcosñipata District: A.C.C.A Predio los Wayqichas	1748	-13.0688	-72.5544
stenotes	USNMENT01118040	J.S. LaPolla	07-Oct-2002	Guyana	Mt. Ayanganna Base Camp	732	5.3344	-59.9248

Table S2: Distribution and trait matrix used in ancestral range and ancestral state reconstructions. A: Neotropical, B: Nearctic, C: Afrotropical, D: Oriental, E: Indo-Australian, F: Australasian, G: Palearctic; Xenococcine associations follow Schneider & LaPolla (2011), numbers in brackets correspond with legend in Fig. 5; * range information for *A. arnoldi* includes distribution (G) of its sister species *A. palearctica*, a species not sampled in the phylogeny.

Species	**Region**	**Mand. teeth**	**Associated xenococcines**
Acropyga acutiventris	DEF	5	*Xenococcus* [I]
Acropyga ambigua	E	5,6	*Xenococcus, Eumyrmococcus* [I,II]
Acropyga arnoldi	CG*	6, 7, 8, 9	*Eumyrmococcus* [II]
Acropyga ayanganna	A	5	*Neochavesia* [III]
Acropyga decedens/goeldii	A	3, 4, 5	*Geococcus, Rhizoecus, Neochavesia, Capitisetella, Dysmicoccus* [III, IV, VI, VII, VIII]
Acropyga donisthorpei	A	5	*Neochavesia* [III]
Acropyga dubitata	A	4	*Rhizoecus* [IV]
Acropyga epedana	B	3, 4	*Rhizoecus* [IV]
Acropyga fuhrmanni	A	4	*Neochavesia* [III]
Acropyga guianensis	A	4, 5	*Neochavesia* [III]
Acropyga hirsutula	A	4, 5	?
Acropyga kinomurai	GE	4	*Xenococcus* [I]
Acropyga lauta	E	5	*Xenococcus, Eumyrmococcus* [I,II]
Acropyga myops	F	5	*Acropygorthezia* [V]
Acropyga butteli	D	5	?
Acropyga pallida	EF	5, 6, 7	*Eumyrmococcus* [II]
Acropyga panamensis	A	4	*Neochavesia* [III]
Acropyga romeo	A	3, 4	?
Acropyga sauteri	D	3, 4	*Eumyrmococcus* [II]
Acropyga sp.	C	4, 5, 6, 7	?
Acropyga silvestrii	C	4, 5, 6, 7	*Rhizoecus* [IV]
Acropyga smithii	A	4	*Geococcus* [VI]
Acropyga stenotes	A	4	*Neochavesia* [III]

Table S3: Dispersal constraints used in ancestral range estimations with RASP. A: Neotropical, B: Nearctic, C: Afrotropical, D: Oriental, E: Indo-Australian, F: Australasian, G: Palearctic. Dispersal probabilities are 1 = geographically abutting ranges, 0.5 = adjacent ranges separated by a body of water, 0.01 = non-adjacent ranges with very low probability of direct faunal exchange.

	A	**B**	**C**	**D**	**E**	**F**	**G**
A	1	1	0.5	0.01	0.01	0.5	0.01
B	1	1	0.01	0.01	0.01	0.01	1
C	0.5	0.01	1	1	0.5	0.5	1
D	0.01	0.01	1	1	1	0.5	1
E	0.01	0.01	0.5	1	1	1	0.01
F	0.5	0.01	0.5	0.5	1	1	0.01
G	0.01	1	1	1	0.01	0.01	1

Table S4: Summary of UCE sequence capture statistics. Table listing the total read count, the total number of recovered contigs, their coverage (X) and average length, and the number of assembled UCE contigs and their average length and coverage.

		All contigs (trimmed)			Contigs aligned to UCE loci		
Taxon	**Total read count (bp)**	**Count**	**Avg. coverage (x)**	**Avg. length (bp)**	**Locus count**	**Avg. length (bp)**	**Avg. coverage (x)**
Acropyga acutiventris_ACR104	2,705,578	34216	16.6	350.8	916	1017.1	145.4
Acropyga acutiventris_ACR23	2,161,633	21539	20.5	371.5	903	998.3	140.1
Acropyga acutiventris_ACR24	2,873,504	55045	12.4	431.1	1014	952.2	118.0
Acropyga acutiventris ACR25	3,072,893	32768	20.0	337.1	908	1057.2	198.2
Acropyga acutiventris_ACR81	511,295	4920	23.2	403.9	827	638.8	49.6
Acropyga acutiventris_ACR82	1,723,356	22590	16.4	333.9	989	847.2	97.1
Acropyga acutiventris_ACR89	2,414,717	28407	16.9	337.7	926	1000.7	127.3
Acropyga ambigua_ACR80	740,836	4702	30.3	456.4	870	862.0	76.1
Acropyga arnoldi_ACR22A	2,518,942	56236	11.4	327.8	1012	1084.3	114.8
Acropyga ayanganna_ACR8	899,213	4850	35.8	522.2	890	912.5	86.1
A. decedens/goeldii_ACR103	1,657,819	11957	26.0	403.2	909	1050.1	117.9
Acropyga donisthorpei_ACR59	1,783,208	24870	16.4	321.2	989	887.5	102.0
Acropyga donisthorpei_ACR85	2,839,303	35413	17.2	322.8	904	1074.0	153.3
Acropyga donisthorpei_ACR86	1,685,975	23806	16.3	314	998	879.0	92.5
Acropyga dubitata_ACR102	540,079	3347	29.8	515.7	883	883.4	51.7
Acropyga epedana_ACR60	1,533,158	10510	26.7	533.2	908	1003.4	119.6
Acropyga epedana_ACR7	735,521	8356	21.1	357.2	933	618.9	66.8
Acropyga fuhrmanni_ACR1	826,407	7884	20.4	426.8	961	876.9	50.4
Acropyga fuhrmanni_ACR2	1,054,093	10354	19.1	406	959	911.0	58.7
Acropyga fuhrmanni_ACR3	1,005,140	9767	21.2	405	969	874.4	69.7
Acropyga fuhrmanni_ACR5	1,053,259	10510	20.8	401	988	889.6	71.1
Acropyga guianensis_ACR21	1,506,476	16200	21.6	354.9	987	860.5	80.8
Acropyga guianensis_ACR50	916,497	9511	23.1	375.5	984	806.0	56.2
Acropyga guianensis_ACR56	2,078,339	18727	24.6	343	890	950.0	137.4
Acropyga hirsutula_ACR57	1,381,313	9833	28.5	412.1	888	950.6	109.3
Acropyga kinomurai_ACR83	1,678,559	23496	16.8	306.8	1024	884.4	106.0
Acropyga lauta_ACR87	551,283	5234	19.6	452.3	944	809.5	45.0
Acropyga lauta_ACR88	1,521,819	12013	21.2	399.3	887	1035.5	103.5
Acropyga myops_ACR26	1,209,776	16513	15.7	351.2	988	906.9	65.8
Acropyga myops_ACR28	1,224,053	16308	15.8	361.3	977	918.8	62.8
Acropyga butteli_ACR100	2,025,030	20786	18.2	340.7	925	1081.7	116.5
Acropyga pallida_ACR27	1,211,227	17716	14.7	318.3	968	896.7	74.9
Acropyga pallida_ACR84	1,885,785	18481	19.9	355	928	993.5	128.2
Acropyga panamensis_ACR51	816,849	9792	19.3	361.2	1003	806.0	46.7
Acropyga romeo_ACR58	1,156,878	17247	18.8	330.6	968	712.5	69.3
Acropyga sauteri_ACR52	856,159	8352	19.0	382.8	978	846.0	55.3
Acropyga silvestrii_ACR101	532,798	4413	22.8	500	848	894.3	44.1
Acropyga sp_ACR90	1,051,482	17043	16.0	283.3	985	658.5	90.0
Acropyga smithii_ACR54	1,393,937	17453	18.2	400.1	983	902.4	73.2
Acropyga smithii_ACR6	776,773	8231	20.4	422.4	959	852.4	51.5
Acropyga stenotes_ACR55	964,788	5816	33.0	439.7	851	918.7	94.0
Agraulomyrmex TZ01	359,942	4383	19.0	357.4	851	479.8	35.8
Anoplolepis gracilipes	764,452	7897	18.5	370.2	918	804.3	57.1
Brachymyrmex sp ACR53	1,199,916	15160	15.8	353.6	1010	786.9	72.0
Camponotus hyatti	2,168,078	44013	12.8	306.7	961	891.3	105.9
Formica moki	2,958,364	77142	12.7	305.5	996	925.2	167.2
Lasius californicus	1,432,247	27370	12.4	317.7	963	870.8	83.1
Myrmecocystus flaviceps	997,124	12137	16.7	325.2	975	846.2	79.9
Nylanderia hystrix	869,609	9570	19.7	359	987	784.8	48.5
Tapinolepis ZA02	1,077,246	18412	13.2	322.5	985	792.2	59.5
Total average	**1,418,055**	**18226**	**19.7**	**375.7**	**945**	**883.7**	**88.5**

Table S5: Comprehensive results of dating analyses and ancestral range reconstructions. Posterior probabilities (PP), median ages, 95% HPD age intervals as estimated by BEAST on the UCE-100 data set, as well as the biogeographic ranges and associated probabilities for each node of the phylogeny as reconstructed by RASP. Node numbers correspond to Fig. 4. A=Neotropical, B=Nearctic, C=Afrotropical, D=Oriental, E=Indo-Australian, F=Australasian, G=Palearctic. Columns Random 1 and Random 2 list median ages and 95% HPD age intervals (in square brackets) as estimated by BEAST on the two randomly selected 100 loci data sets. N/a means node is not present in the resulting MCC tree.

Node	Age - mean	Age - 95%	Range	Range - PP	Random 1	Random 2
24	13.95	7.82,21.0	C	100	14.37[8.45,21.37]	15.95[8.68,23.48]
25	14.67	8.48,22.13	C	100	15.19[9.1, 22.25]	18.03[10.97,25.87]
26	14.31	8.26,20.89	EF	58.38	14.21[8.48, 20.65]	13.84[8.41,19.81]
			E	41.62		
27	17.06	10.77,24.09	DE	48.76	n/a	n/a
			DEF	48.3		
			DF	1.97		
			E	0.89		
			F	0.09		
28	16.75	10.3,23.56	DEF	90.94	16.84[10.74,23.38]	n/a
			DF	5.94		
			DE	2.53		
			EF	0.27		
			E	0.25		
			F	0.06		
29	18.63	12.0,26.01	DEF	66.83	17.99[11.9,25]	16.77[10.99,23.22]
			DE	27.23		
			D	3.05		
			DF	2.08		
			E	0.56		
			EF	0.21		
			F	0.06		
30	21.43	14.27,29.25	DE	52.58	20.85[13.92,28.35]	20.12[13.42,27.92]
			DEF	38.17		
			D	8.76		
			E	0.34		
			DF	0.15		
31	19.48	10.29,29.17	E	71.07	20.68[13.18,29.03]	20.66[13.21,28.82]
			EG	25.15		
			DE	1.96		
			DEG	1.69		
			CEG	0.13		
32	27.72	19.6,36.53	E	62.26	27.26[19.23,35.99]	26.34[18.1,34.84]
			EG	17.85		
			DE	13.74		
			D	5.31		
			DEG	0.37		

Node	Age - mean	Age - 95%	Range	Range - PP	Random 1	Random 2
			DG	0.2		
			EF	0.07		
			CDE	0.05		
			DF	0.02		
			CD	0.02		
			DEF	0.01		
33	28.4	20.36,37.63	CE	65.56	27.59[19.46,36.4]	28.03[19.85,36.98]
			CEG	17.41		
			CDE	10.34		
			CD	6.21		
			CDG	0.3		
			D	0.1		
			CDF	0.03		
			CEF	0.03		
			C	0.01		
			CF	0.01		
34	13.65	7.9,20.1	A	100	14.66[8.78,21.03]	n/a
35	13.9	8.53,19.83	A	100	13.68[8.34,19.59]	n/a
36	7.12	3.91,11.13	AB	96.68	7.66[4.3,11.53]	n/a
			A	3.32		
37	8.82	5.2,13.36	A	70.05	8.85[5.33,13.03]	n/a
			AB	29.95		
38	12.44	7.54,18.13	A	99.71	12.97[8.44,18.31]	n/a
			AB	0.29		
39	14.31	9.39,20.19	A	100	14.83[9.72,20.49]	n/a
40	18.52	12.72,25.07	A	100	18.63[12.92,25.47]	n/a
41	22.06	14.68,30.75	A	100	21.78[15.18,29.32]	n/a
42	14.84	9.15,21.86	A	100	15.32[8.81,22.41]	16.32[9.28,24.28]
43	16.43	9.65,25.89	A	100	15.93[9.43,23.27]	n/a
44	27.76	18.54,38.81	A	100	26.64[18.83,35.36]	28.03[19.8,37.37]
45	30.57	21.52,40.19	ACE	84.6	28.76[20.29,37.89]	30.61[22.04,40.88]
			ACD	8.72		
			AEG	5.61		
			ADE	0.36		
			AD	0.28		
			AC	0.19		
			ACG	0.15		
			ADG	0.05		
			ACF	0.03		
			AE	0.01		
46	22.52	13.82,32.38	n/a	n/a	24.87[15.4,34.87]	24.94[15.83,34.76]
47	46.52	36.25,58.1	n/a	n/a	46.11[36.19,57.6]	45.99[36.31,57.37]

Table S6: Comprehensive results of ancestral state reconstructions under the ER model. Shown are probabilities of each state for Xenococcine associations and number of mandibular teeth. Node numbers correspond to Figs 4 and 5. Xenococcine associations: I: *Xenococcus*, II: *Eumyrmococcus*, III: *Neochavesia*, IV: *Rhizoecus*, V: *Acropygorthezia*, VI: *Geococcus*, VII: *Capitisetella*, VIII: *Dysmicoccus.* Bolded numbers highlight the most probable state reconstruction. Node numbers correspond to Fig. 5.

	Xenococcine association								number of mandibular teeth						
Node	**I**	**II**	**III**	**IV**	**V**	**VI**	**VII**	**VIII**	**3**	**4**	**5**	**6**	**7**	**8**	**9**
24	0.047	**0.690**	0.046	0.173	0.011	0.011	0.011	0.011	0.001	0.196	**0.460**	0.168	0.168	0.003	0.003
25	0.048	**0.732**	0.046	0.137	0.009	0.009	0.009	0.009	0.001	0.195	**0.460**	0.167	0.167	0.005	0.005
26	0.112	**0.877**	0.003	0.001	0.006	0.001	0.001	0.001	0.000	0.000	**0.993**	0.007	0.001	0.000	0.000
27	0.128	**0.849**	0.006	0.002	0.013	0.001	0.001	0.001	0.000	0.000	**1.000**	0.000	0.000	0.000	0.000
28	0.130	**0.845**	0.006	0.002	0.014	0.001	0.001	0.001	0.000	0.000	**1.000**	0.000	0.000	0.000	0.000
29	0.143	**0.834**	0.008	0.002	0.009	0.001	0.001	0.001	0.000	0.006	**0.993**	0.000	0.000	0.000	0.000
30	0.132	**0.840**	0.015	0.003	0.006	0.001	0.001	0.001	0.005	0.213	**0.779**	0.001	0.001	0.001	0.001
31	0.419	**0.522**	0.030	0.008	0.005	0.005	0.005	0.005	0.001	0.283	**0.709**	0.002	0.002	0.001	0.001
32	0.155	**0.726**	0.095	0.013	0.004	0.003	0.002	0.002	0.000	0.274	**0.723**	0.001	0.001	0.000	0.000
33	0.134	**0.707**	0.128	0.018	0.004	0.003	0.003	0.003	0.000	0.280	**0.716**	0.002	0.002	0.000	0.000
34	0.000	0.001	**0.995**	0.001	0.000	0.001	0.000	0.000	0.000	**0.983**	0.017	0.000	0.000	0.000	0.000
35	0.004	0.006	**0.905**	0.029	0.003	0.047	0.003	0.003	0.000	**1.000**	0.000	0.000	0.000	0.000	0.000
36	0.000	0.000	0.024	**0.971**	0.000	0.002	0.001	0.001	0.005	**0.995**	0.000	0.000	0.000	0.000	0.000
37	0.000	0.000	0.030	**0.964**	0.000	0.002	0.001	0.001	0.000	**1.000**	0.000	0.000	0.000	0.000	0.000
38	0.009	0.011	0.338	**0.598**	0.009	0.016	0.010	0.010	0.000	**1.000**	0.000	0.000	0.000	0.000	0.000
39	0.010	0.013	**0.508**	0.420	0.010	0.019	0.010	0.010	0.000	**1.000**	0.000	0.000	0.000	0.000	0.000
40	0.003	0.008	**0.917**	0.048	0.002	0.019	0.002	0.002	0.000	**0.999**	0.000	0.000	0.000	0.000	0.000
41	0.003	0.011	**0.966**	0.013	0.001	0.005	0.001	0.001	0.000	**0.974**	0.025	0.000	0.000	0.000	0.000
42	0.000	0.000	**0.999**	0.000	0.000	0.000	0.000	0.000	0.001	0.198	**0.799**	0.001	0.001	0.001	0.001
43	0.000	0.001	**0.998**	0.000	0.000	0.000	0.000	0.000	0.000	0.196	**0.802**	0.000	0.000	0.000	0.000
44	0.011	0.054	**0.918**	0.009	0.002	0.003	0.002	0.002	0.000	0.326	**0.671**	0.001	0.001	0.000	0.000
45	0.082	0.414	**0.461**	0.017	0.007	0.007	0.006	0.006	0.001	0.300	**0.696**	0.002	0.002	0.000	0.000

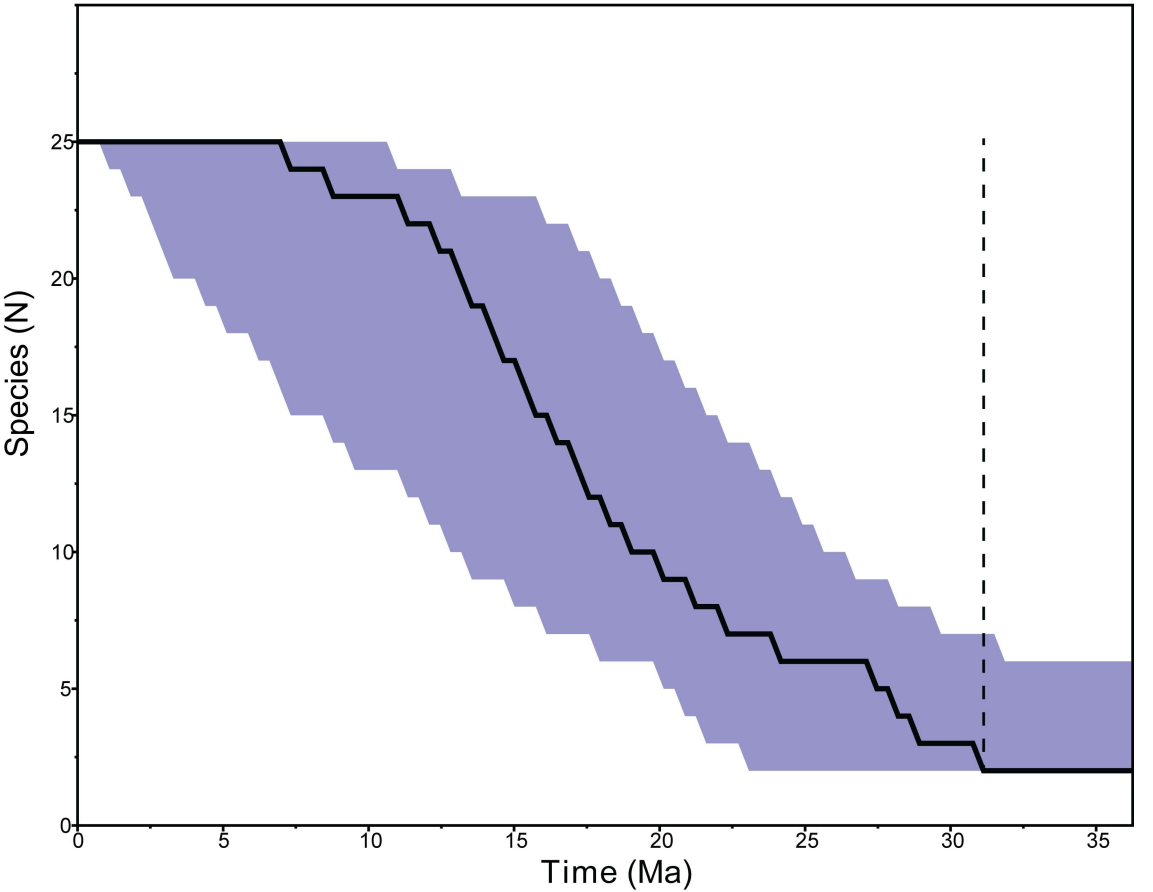

Figure S1: *Acropyga* lineages through time. Lineage through time plots as estimated with Tracer v1.6 from a posterior distribution of 55793 trees. Dotted line indicates the most recent common ancestor of *Acropyga.*

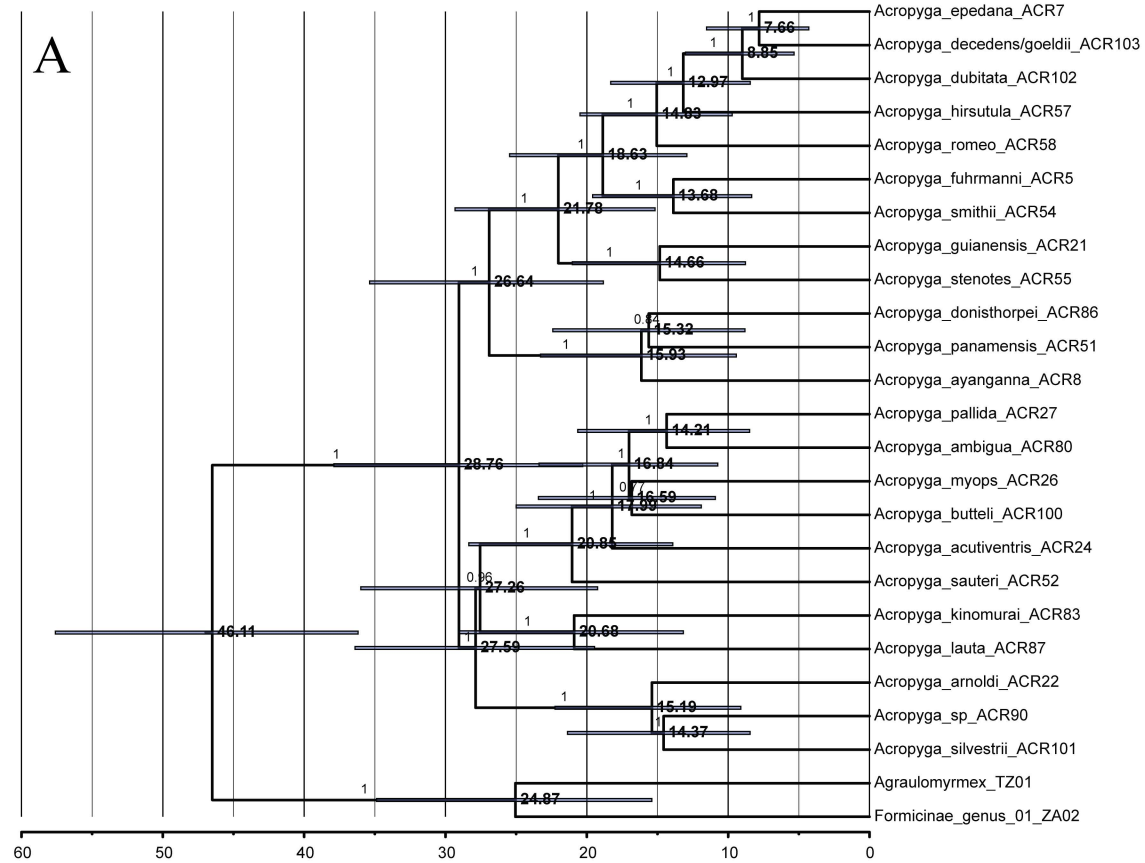

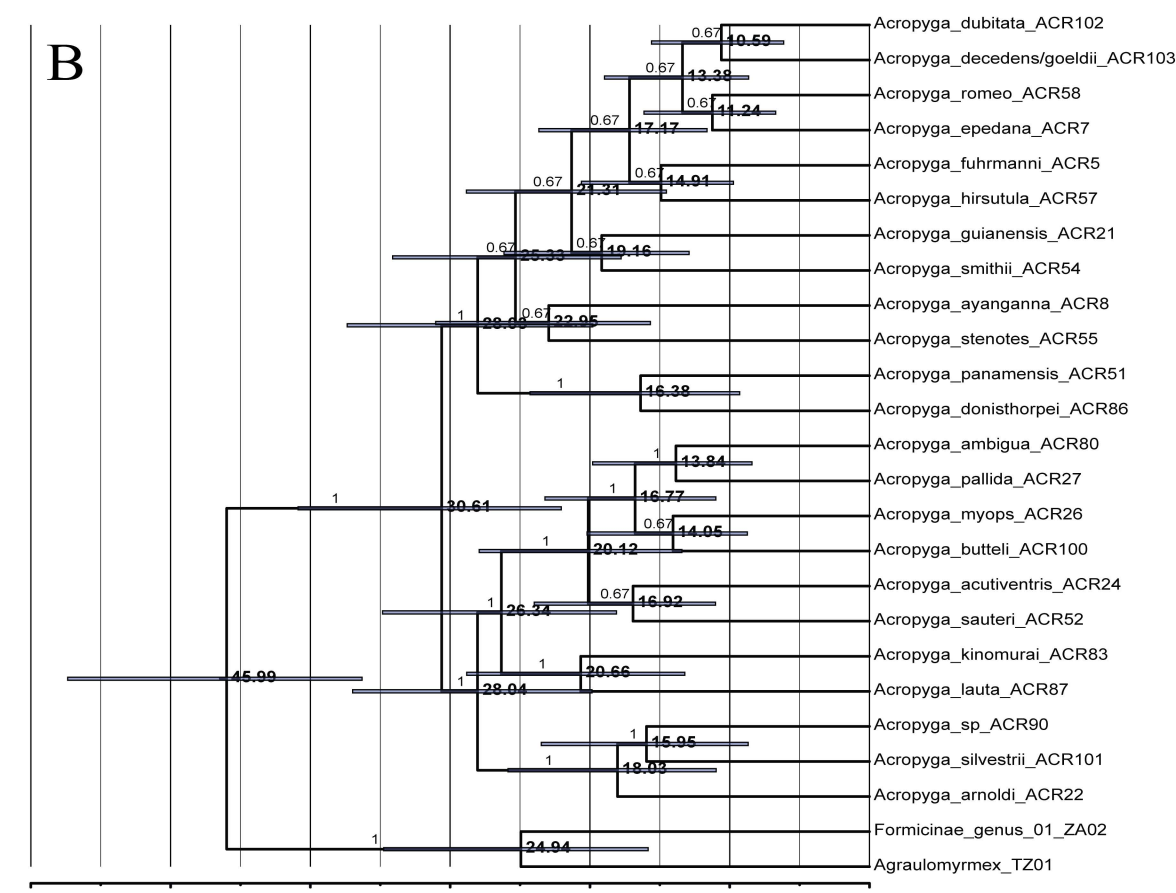

Figure S2: MCC **trees resulting from BEAST analyses on 100 randomly selected loci**. A: set random 1, summarizing 40000 trees; B: set random 2, summarizing 25000 trees.